THE INFLUENCE OF HYDRAULIC LOADING RATE ON NITRIFICATION PERFORMANCE IN A TWO STAGE BIOLOGICAL AERATED FILTER PILOT SYSTEM

by

Kari J. Husovitz

Thesis submitted to the Faculty of
Virginia Polytechnic Institute and State University
in partial fulfillment of the requirements for the degree of

Master of Science
in
Environmental Engineering

APPROVED:

_____	_____
Dr. Nancy G. Love, Co-chair	Dr. John C. Little, Co-chair

_____
Dr. John T. Novak

December 2, 1998
Blacksburg, VA

Keywords: biofiltration, nitrification, flow rate, wastewater, mass transfer

THE INFLUENCE OF HYDRAULIC LOADING RATE ON NITRIFICATION PERFORMANCE IN A TWO STAGE BIOLOGICAL AERATED FILTER PILOT SYSTEM

by

Kari J. Husovitz

ABSTRACT

A two-stage (carbon oxidation stage one, ammonia oxidation stage two) biological aerated filter was operated for 10 months on-site at a domestic wastewater treatment plant. Over the study, the system was operated at different hydraulic loading rates that resulted in a range of applied organic and ammonia mass loadings. Performance was monitored regularly for water quality parameters in the effluent and along the length of the reactors. It was found that nitrification performance was significantly influenced by organic loading rates greater than 1.2 kg $cBOD_5/m^3$-d. Additional experiments were conducted in which a constant mass of ammonia was applied (Phase 1: 1.40 ± 0.08 kg NH_3-N/m^3-d; Phase 2: 1.31 ± 0.02 kg NH_3-N/m^3-d) to the N column, the second stage of the system, over a range of hydraulic loading rates (5.1 - 15.8 m/h). Phases of testing were defined by the background hydraulic loading rate applied to the system (Phase 1: 8.3 m/h; Phase 2: 7.1 m/h) at which the reactors were allowed to reach a steady effluent quality for at least one week prior to testing. Organic loading was minimized and kept relatively constant throughout the hydraulic loading rate experiments (0.65 ± 0.2 kg $cBOD_5/m^3$-d) in order to obtain an evaluation of nitrification capacity with minimal competition from heterotrophic bacteria. Results indicated that nitrification performance improved by 17% as the applied velocity increased over the indicated range. A steady-state biofilm model capable of predicting substrate flux was applied to the data in an attempt to explain the improvement in performance with hydraulic loading rate from a fundamental standpoint. Mass transfer coefficients, K_L, were derived from the model for conditions in which the experimentally observed flux correlated with the model predictions. Derived K_L values were lower than estimations offered by correlation equations but increased with velocity at a similar rate. The model failed to account for changes that may have occurred in biofilm kinetics and structure throughout the length of the reactor.

ACKNOWLEDGMENTS

I would like to extend many thanks to my committee members, Drs. Nancy Love, John Little, and John Novak, for their active contributions throughout this project. My research efforts could not have been a success without their time, energy, creativity, experience and organization.

Special thanks is also extended to Troy Holst of Infilco Degremont, Inc. for the countless hours he spent with the pilot units and with our project team. I also appreciate the contributions of others at IDI, including Martin Bucher, Steve Tarallo and Temple Ballard.

I would alike to recognize Julie Petruska and Jodi Smiley for the much-needed guidance they provided in the laboratory. Their help and experience is greatly appreciated.

My utmost gratitude is given to my co-workers on this project, Kevin Gilmore and Arnaud Delahaye, for their help, patience, encouragement, and most importantly, their humor. I also thank Ken Woodard and Monica Mace, undergraduates at Virginia Tech, for their help in the lab.

Finally, I offer special thanks to my friends and family, both at home and in the NEB, for their support and patience throughout this project.

TABLE OF CONTENTS

LIST OF FIGURES

Literature Review

Manuscript

LIST OF TABLES

Manuscript

LITERATURE REVIEW

Fixed Film Processes

In recent years there has been a significant increase in the use of fixed-film, or attached growth, processes to treat municipal and industrial wastewater. A fixed-film system is a biological treatment process in which the microorganisms responsible for the removal of organic pollutants in wastewater are attached to an inert medium such as rocks or plastic material (Metcalf and Eddy, 1991). Examples of fixed-film processes include trickling filters, rotating biological contactors (RBCs), and biological aerated filters (BAFs). Fixed-film processes offer several advantages over the conventional biological treatment process of activated sludge, which employs a suspended growth reactor followed by a secondary clarifier, that have led to the increase in fixed-film research and application. One of the most important advantages is the high concentration of biomass that can be maintained in a fixed-film process, which leads to a smaller required reactor footprint. This is very attractive to existing wastewater treatment plants that require upgrades but offer very little land area in which to expand. Biofilms have also been noted to offer a more stable biological process than activated sludge (Kugaprasathan et al., 1992), in that shock loads can be handled more effectively. Lastly, by combining the slow growth rates of nitrifying bacteria with an attached growth system, biofilm processes have been shown to be efficient in ammonia removal (Carrand et al., 1990; Peladan et al., 1996; Rogalla et al., 1990).

Nitrification

There is an increasing demand for wastewater treatment systems to remove nutrients in the form of nitrogen from the wastewater stream. Nitrogen, when discharged in excess to a receiving stream, can lead to undesirable water quality conditions, including low dissolved oxygen concentrations and algae blooms. Additonally, nitrogen in the form of reduced ammonia (NH_4^+-N) is toxic to fish. One of the most common means of removing ammonia from wastewater is through biological nitrification. The nitrification process contributes to nitrogen removal by transforming ammonia to a more oxidized form of nitrogen such as

nitrite (NO_2^-) or nitrate (NO_3^-). Nitrification is a two-step process where ammonia oxidizing bacteria (AOB) oxidize ammonia to nitrate, and nitrite oxidizing bacteria (NOB) convert nitrite to nitrate. Nitrifying bacteria, classified as autotrophs, differ from those bacteria that remove carbonaceous material, known as heterotrophs. Autotrophs grow much slower than heterotrophs and are out-competed by heterotrophs when both organic carbon and ammonia substrates are present. Nitrifiers are also more sensitive to environmental changes such as pH and temperature (Beg et al, 1995).

Biological Aerated Filters

The biological aerated filter (BAF) is among the latest innovations in fixed-film processes. BAFs are high-rate, upflow or downflow fixed-film systems that incorporate submerged media responsible for supporting biofilm growth and filtering unwanted suspended solid material. BAFs have been successfully used for carbon oxidation, nitrification (conversion of ammonia to nitrate) and denitrification (conversion of nitrate to nitrogen gas). (Carrand et al., 1990; Pujol et al., 1994; Stensel et al., 1988). In addition to offering a compact biological treatment process, BAFs eliminate the need for secondary clarifiers, making them independent of sludge settling issues that often govern the operation of activated sludge systems. They also lack foul odors because only treated effluent is exposed to the air. Lastly, BAF systems can operate successfully under much higher hydraulic and organic loading rates when compared to typical activated sludge systems (Metcalf and Eddy, 1991; Stensel et al., 1988).

Despite the many advantages that BAF systems seem to offer, widespread acceptance has been limited in the United States. However, many pilot-scale investigations and full-scale case studies have been conducted to evaluate BAF performance . In 1988 as part of a demonstration project sponsored by the U.S. Environmental Protection Agency (EPA), a full-scale BAF module was conceived to evaluate basic design criteria, performance and operational needs. (Stensel et al., 1988). The module had a nominal capacity of 0.5 MGD and was operated for a two year period on wastewater that consisted of 70-80% domestic sewage with minor contributions from various industries. The pilot system described in the study

by Stensel et al. (1988) is similar to the study presented here in media type and height, aeration, backwash sequence and frequency, and influent characteristics, but differed in reactor surface area and influent application (downflow rather than upflow). The study by Stensel et al. (1988) resulted in guidelines for a wide variety of operating parameters, such as backwash frequency, average soluble organic loadings, oxygen requirements and sludge production. Rogalla et al. (1990) explored ammonia nitrogen removal with BAFs. It was found that nitrification could be achieved in the BAF but only when carbonaceous load to the filter was limited. Consistent ammonia removal above 90% occurred when the organic load was kept below 1.5 kg/m^3-d. Rogalla et al. (1990) also summarized the operational parameters and performance characteristics of a full-scale nitrifying BAF system in Luneville, France.

Many articles have been published that summarize full-scale system operation of the Biofor™, a BAF manufactured by Infilco Degremont, Inc. (IDI, Richmond, VA) (Carrand et al., 1990; Pujol et al., 1994; Sagberg et al., 1992). Additionally, Degremont, the parent company of IDI, has also conducted pilot-scale experiments on the Biofor™. One particular study evaluated the upper operating limits of the Biofor™ process in terms of upflow water velocity (Peladan et al., 1996). They concluded that an increase in water velocity has a positive effect on nitrification and found that nitrification could occur successfully at velocities as high as 30 m/h. Because the pilot system in the study by Peladan et al. (1996) involved the use of synthetic wastewater that did not contain organic carbon or suspended solid matter, the authors acknowledged the need for further research to explore the influence of these pollutants on nitrification capacity.

Mass Transfer

Substrate utilization by biofilms can be simply described by three main steps, 1) transfer of the substrate from the bulk liquid to the external biofilm surface, 2) diffusion of the substrate within the biofilm, and 3) substrate consumption by the microorganisms within the biofilm (Zhang and Bishop, 1994). According to Zhang et al. (1994), although step 1 is purely physical under the assumption that no substrate

is used prior to reaching the biofilm, it is a very important step because, under steady state conditions, the rate of the overall reaction resulting from steps 2 and 3 is always equal to step 1. Mass transfer, such as that which occurs in the stagnant liquid film that separates the bulk liquid from the biofilm, is governed by Fick's first law which says that mass flux (flow per unit area per time) is proportional to the concentration gradient across the bulk liquid/biofilm boundary layer. Mass transfer in biofilms is conventionally described by molecular diffusion, which results from the random molecular motion of molecules in a fluid. If a concentration gradient exists, then the molecules will move in the direction toward the lower concentration at a flux defined by the concentration gradient. Figure 1 and Equation 1 below describe pure diffusive mass transfer.

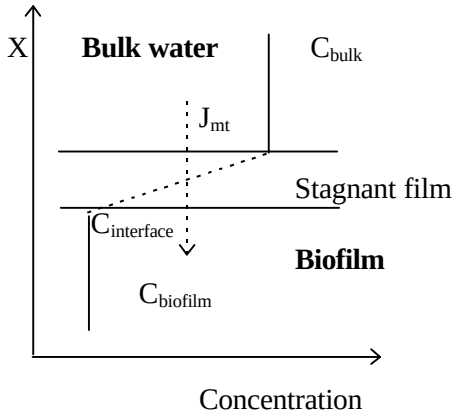

Figure 1. Conceptual schematic of diffusive mass transfer across the bulk liquid/biofilm boundary layer..

$$J = -\frac{D}{L}\left(C_{bulk} - C_{interface}\right) \qquad \text{[Eq. 1]}$$

where L = stagnant film thickness [L]
D = molecular diffusion coefficient [L^2T^{-1}].
J = mass flux of substrate [$ML^{-2}T^{-1}$]

Mass transfer is influenced by turbulent conditions that often exist in the bulk liquid of real biofilm systems. Eq. 2 below describes turbulent mass transfer, where, by analogy to Eq. 1, the mass transfer

coefficient, K_L, is defined as D/L. The thickness of the stagnant film depends on the hydraulic conditions of flow past the film, as higher turbulence results in a thinner film (Christiansen et al., 1995). The mass transfer coefficient is related to the film thickness; the thinner the film, the greater the mass transfer coefficient, the faster the mass transfer flux.

$$J = -K_L\left(C_{bulk} - C_{interface}\right) \qquad \text{[Eq. 2]}$$

Research efforts have attempted to measure both mass transfer coefficients and the stagnant film thickness (Horn and Hempel, 1995; Land and Lewankowski, 1995; Zhang and Bishop, 1994) in biofilm systems. Because both parameters require micro-level measurements, these measurements are often done in controlled laboratory conditions suited for using microelectrodes. One means of characterizing the external mass transfer is with the concentration boundary layer (CBL), which could be defined as the distance from the surface of the biofilm through the bulk liquid in which there is a concentration gradient, implying that diffusion of the substrate into the biofilm is occurring (Zhang and Bishop, 1994). The CBL is analogous to the diffusion layer. One of the most common substrates in CBL investigations is dissolved oxygen which can be measured with a microelectrode. Zhang and Bishop (1994) investigated the dissolved oxygen CBL under different conditions in a biofilm system and demonstrated the effects on mass transfer resistance. The biofilm system consisted of a flat plate supporting biofilm growth in an open flow channel. Their experimental results indicated that at a) an increasing substrate loading rate, b) an increasing fluid velocity, and c) an increasing roughness of biofilm surface, external mass transfer resistance decreased. Horn and Hempel (1995) conducted a similar investigation using microelectrodes to measure the dissolved oxygen profiles at biofilm surfaces. A comparison of their measured mass transfer coefficients with values given by a correlation equation showed poor correlation. Horn and Hempel (1995) concluded that the mass transfer coefficient given as a quotient of the diffusion coefficient through the boundary layer thickness (D/L) is an oversimplification because it is likely that the biofilm structure changes with flow conditions.

This conclusion was in agreement with a study conducted by Kugaprasathanm et al. (1992) in which the effect of turbulent conditions on nitrifying biofilms was investigated. It was shown that an increase in turbulence changes the filament-like structure of the biofilm and increases the mass flux into the biofilm. Finally, by measuring dissolved oxygen concentrations at locations in the biofilm that varied both horizontally and vertically, Yang and Lewandowski (1995) were able to use mass transfer coefficient measurements to illustrate the irregularity of biofilm structure.

It is not always necessary to measure diffusion layer thickness and interfacial concentrations to estimate mass transfer coefficients. Numerous correlation equations based on a variety of reactor configurations are offered in the literature (Christiansen et al., 1995; Grady et al, 1999; Weber and Smith, 1987; Zhang and Bishop, 1994). Correlation equations are often based upon the dimensionless Sherwood number, Sh, which represents the ratio of turbulent diffusion to molecular diffusion for a given system. The definition of Sh and its relationship to K_L are given in Eq. 3.

$$= \frac{K_L d}{L} \qquad \text{[Eq. 3]}$$

$$D_L$$

Biofilm Modeling Concepts

Biofilms play a significant role in biological wastewater treatment, specifically in fixed-film, or aerated filters (BAFs). Design and operation of fixed-film treatment systems are based primarily on experience and empirical relationships. However, research conducted over the last twenty years has biofilm treatment systems. The conceptual basis for many biofilm models is illustrated in Figure 2. This figure represents the perspective of one-dimensional biofilm models in which all property gradients (such as

surface (Picioreanu, 1998; Wanner, 1995). The main principles that govern substrate removal in the majority of one-dimensional biofilm models are 1) diffusion of substrate from the bulk solution to the biofilm surface, and 2) simultaneous biological reaction and diffusion within the biofilm (Saez and Rittmann, 1987). In other words, the biofilm is treated in these types of models as "a slab of uniform material reacting with a diffusing substrate" (Hermanowicz, 1998).

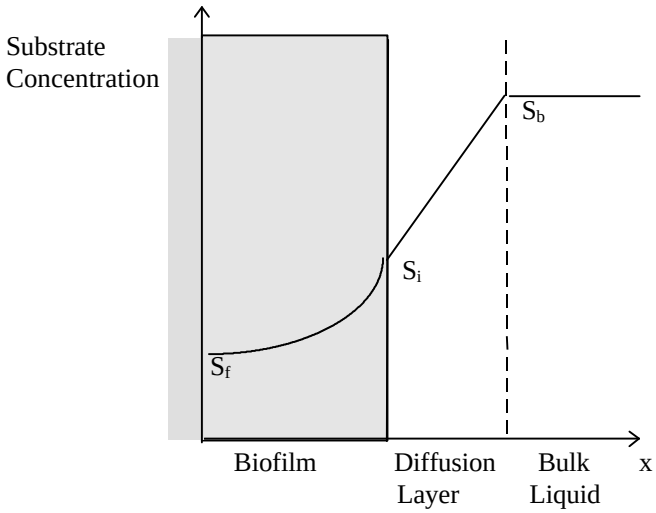

Figure 2. Conceptual basis for one-dimensional biofilm models, showing substrate concentration profiles and coordinate system. (Adapted from Saez and Rittmann, 1987)

Biological reaction carried out in biofilms is often described by the empirical Monod relationship (Grady et al., 1999)

$$\mu = \mu_{max} \frac{S}{K_s + S} \qquad \text{[Eq. 4]}$$

where μ = specific growth rate [T^{-1}]
μ_{max} = maximum specific growth rate [T^{-1}]
S = growth limiting substrate concentration [ML^{-3}]
K_s = half saturation constant, substrate concentration at half the maximum growth rate [ML^{-3}].

The Monod growth rate constant has been used in zero, mixed, and first order reaction rate equations when describing biofilm kinetics. If the substrate concentration in the biofilm, S_f, is sufficiently greater than K_s, then the reaction can be describe by zero-order kinetics, where the rate of reaction is no longer influenced

by the substrate concentration. On the contrary, if S_f is sufficiently lower than K_s, the reaction rate is first order with respect to substrate concentration. Additionally, biofilms can be classified by the extent to which the substrate penetrates the biofilm. A fully penetrated biofilm is one in which S_f changes so little from S_i, the concentration at the bulk liquid/biofilm interface, that the specific utilization rate is the same as if all the biomass were exposed to a concentration S_i. A deep biofilm is one in which S_f approaches zero. Since it is possible that first or zero-order biofilms can be either deep or fully-penetrated, mixed order reactions rates are also used (Saez and Rittmann, 1990). It is obvious that when a substrate fully penetrates a biofilm, the substrate utilization is being limited by the reaction rate. However, if a substrate only partially penetrates the biofilm, reaction is occurring at a maximum rate, implying that conditions are limited by the rate of substrate diffusion (Williamson and McCarty, 1976).

The first comprehensive biofilm model was offered by Williamson and McCarty (1976). The model was based on single substrate limitation, utilized Monod kinetics and considered substrate diffusion through the bulk solution to the biofilm as well as simultaneous substrate diffusion and biological reaction in the biofilm. Later, this model was expanded by Rittmann and McCarty (1980) to include the concepts of biofilm growth and loss and a minimum bulk substrate concentration necessary to support the biofilm. One difficulty in using the equations that describe simultaneous substrate utilization and diffusion in the biofilm is that the non-linearity of the reaction equations cannot be integrated to obtain an analytical solution. Therefore, Saez and Rittman (1987) later developed a pseudo-analytical solution for steady state biofilm kinetics. Biofilm thickness and substrate flux into the biofilm can be obtained from algebraic equations incorporating kinetic and physical parameters and bulk substrate concentration.

The recent application of the confocal scanning laser microscope (CSLM) to the study of biofilms has produced new revelations about biofilm structure that have led to a reevaluation of conceptual models (Costerton, 1995; Hermanowicz, 1998). The non-destructive, in situ observations revealed through CSLM show a great variety in biofilm structure ranging from homogeneous layers to mushroom- or tulip-shaped clusters, or microcolonies. Thus, new three-dimensional perspectives of biofilms are emerging. These

revelations about the heterogeneous structure of biofilms imply a contradicting concept of the influence of abiotic factors such as water flow compared to that depicted in Figure 1, where only the outermost biofilm surface is exposed to liquid flow (Costerton, 1995; Hermanowicz, 1998). This implies that advective transport, not just diffusion, may act as a significant transport mechanism in biofilm systems (Horn and Hempel, 1997).

Because it is now known that there is significant variability in biofilm structure, new modeling efforts in two and even three dimensions are being attempted (Hermanowicz, 1998; Picioreanu et al., 1998; Wanner, 1995). It has been suggested that one-dimensional models can be adequate for biofilm description (Bishop and Rittmann, 1996), but if structural properties are to be predicted, multidimensional modeling may be required (Picioreneau et al., 1998). Structural biofilm properties may be important on an operational level. Picioreneau et al. (1998) offer a discrete-differential model of biofilm structure which suggests that biofilm surface area and density changes with Reynolds number, or bulk fluid velocity. They suggest that the increased velocity not only reduces the thickness of the boundary resistance layer, but it also has a smoothing effect on the biofilm surface. This may imply that a larger biofilm surface area is exposed to the bulk substrate concentration at higher bulk flow velocities.

REFERENCES

Beg., S.A., Hassan, M.M., Chaudry, A.S. (1995). Multi-substrate analysis of carbon oxidation and nitrification in an unpflow packed-bed biofilm reactor. *J. Chem. Tech. Biotechnol*., **64**, 367-378.

Bishop, P. and Rittmann, B.E. (1996). Modeling heterogeneity in biofilms: Report of the discussion session. *Wat. Sci. Tech*., **32**, 263-265.

Carrand, G., Capon, B., Rasconi, A., Brenner, R. (1990). Elimination of carbonaceous and nitrogenous pollutants by a twin-stage fixed growth process. *Wat. Sci. Tech*., **22**, 261-272.

Christiansen, P., Hollesen, L., Harremoes, P. (1995). Liquid film diffusion on reaction rate in submerged biofilters. *Wat. Res*., **29**, 947-952.

Costerton, J.W. (1995). Overview of microbial biofilms. *Journal of Industrial Microbiology*, **15**, 137-140.

Grady, C.P.L., Jr., Daigger, G.T., Lim, H.C. (1999). *Biological Wastewater Treatment*. Marcel Dekker, Inc. New York.

Hermanowicz, S.W. (1998). Two-dimensional simulations of biofilm development: Effects of external environmental conditions. *Proceedings of the IAWQ Specialty Conference on Microbial Ecology of Biofilms: Concepts, Tools and Applications*, Lake Bluff, IL, 136-143.

Horn, H. and Hempel, D.C. (1995). Mass transfer coefficients for an autotrophic and a heterotrophic biofilm system. *Wat. Sci. Tech*., **32**, 199-204.

Horn, H. and Hempel, D.C. (1997). Modeling mass transfer and substrate utilization in the boundary layer of biofilm systems. *Proceedings of the Second International Conference on Microorganisms in Activated Sludge and Biofilm Processes*, Berkeley, CA, 103-110.

Kugaprasathan, S., Nagaoka, H., Ohgaki, S. (1992). Effect of turbulence on nitrifying biofilms at non-limiting substrate conditions. *Wat. Res*., **26**, 1629-1638.

Metcalf and Eddy, Inc. (1991). Wastewater Engineering: Treatment, Disposal and Reuse. 3rd edition. McGraw Hill, Inc., New York, NY.

Peladan, J.G., Lemmel, H., Pujol, R. (1996). High nitrification rate with upflow biofiltration. *Wat. Sci. Tech*., **34**, 347-353.

Picioreanu, C., van Loosdrecht, M.C.M., Heijnen, J.J. (1998). Discrete-differential modeling of biofilm structure. *Proceedings of the IAWQ Specialty Conference on Microbial Ecology of Biofilms: Concepts, Tools and Applications*, Lake Bluff, IL, 144-151.

Pujol., R., Hamon, M., Kandel, X., Lemmel, H. (1994). Biofilters: Flexible, reliable biological reactors. *Wat. Sci,. Tech*., **29**, 33-38.

Rittmann, B.E. and McCarty, P.L. (1981). Substrate flux into biofilms of any thickness. *J. Evniron. Engr.*,**107**, 831-847.

Rogalla, F., Payraudeau, M., Bacquet, G., Bourbigot, M., Sibony, J., Gilles, P. (1990). Nitrification and phosphorus precipitation with biological aerated filters. *Journal WPCF*, **62**, 169-176.

Saez, P. and Rittman, B.E. (1987). Improved pseudoanalytical solution for steady-state biofilm kinetics. *Biotechnol. Bioeng.*, **32**, 379-385.

Saez, P. and Rittmann, B.E. (1990). Error analysis of limiting-case solutions to the steady-state biofilm model. *Wat. Res.*, **24**, 1181-1185.

Sagberg, P., Dauthuille, P., Hamon, M. (1992). Biofilm reactors: A compact solution for the upgrading of wastewater treatment plants. *Wat. Sci. Tech.*, **26**, 733-742.

Stensel, H.D., Brenner, R.C., Lee, K.M., Melcer, H., Rakness, K. (1988). Biological filter evaluation. *J. Evniron. Engr.*, **114**, 655-671.

Wanner, Oskar. (1995). New experimental findings and biofilm modeling concepts. *Wat. Sci. Tech.*, *32*, 133-140.

Weber, W.J., and Smith, E.H. (1987). Simulation and design models for adsorption processes. *Environ. Sci. Technol.*, **21**, 1040-1050.

Williamson K. and McCarty, P.L. (1976) A model of substrate utilization by bacterial films. *Journal WPCF*, **48**, 9-23.

Yang, S. and Lewandowski, Z. (1995). Measurement of local mass transfer coefficients in biofilms. *Biotechnol. Bioeng.*, **48**, 737-744.

Zhang, T.C. and Bishop, P.L. (1994). Experimental determination of the dissolved oxygen boundary layer and mass transfer resistance near the fluid-biofilm interface. *Wat. Res.*, **30**, 47-58.

THE INFLUENCE OF HYDRAULIC LOADING RATE ON NITRIFICATION PERFORMANCE IN A TWO-STAGE BIOLOGICAL AERATED FILTER PILOT SYSTEM.

Kari J. Husovitz, Nancy G. Love, John C. Little

Submitted to Water Environment Research

ABSTRACT

A two-stage (carbon oxidation stage one, ammonia oxidation stage two) biological aerated filter was operated for 10 months on-site at a domestic wastewater treatment plant. Over the study, the system was operated at different hydraulic loading rates that resulted in a range of applied organic and ammonia mass loadings. Performance was monitored regularly for water quality parameters in the effluent and along the length of the reactors. It was found that nitrification performance was significantly influenced by organic loading rates greater than 1.2 kg $cBOD_5/m^3$-d. Additional experiments were conducted in which a constant mass of ammonia was applied (Phase 1: 1.40 ± 0.08 kg NH_3-N/m^3-d; Phase 2: 1.31 ± 0.02 kg NH_3-N/m^3-d) to the N column, the second stage of the system, over a range of hydraulic loading rates (5.1 - 15.8 m/h). Phases of testing were defined by the background hydraulic loading rate applied to the system (Phase 1: 8.3 m/h; Phase 2: 7.1 m/h) at which the reactors were allowed to reach a steady effluent quality for at least one week prior to testing. Organic loading was minimized and kept relatively constant throughout the hydraulic loading rate experiments (0.65 ± 0.2 kg $cBOD_5/m^3$-d) in order to obtain an evaluation of nitrification capacity with minimal competition from heterotrophic bacteria. Results indicated that nitrification performance improved by 17% as the applied velocity increased over the indicated range. A steady-state biofilm model capable of predicting substrate flux was applied to the data in an attempt to explain the improvement in performance with hydraulic loading rate from a fundamental standpoint. Mass transfer coefficients, K_L, were derived from the model for conditions in which the experimentally observed flux correlated with the model predictions. Fitted K_L values were lower than estimations offered by correlation equations but increased with velocity at a similar rate. The model failed to account for changes that may have occurred in biofilm kinetics and structure throughout the length of the reactor.

INTRODUCTION

Biological aerated filtration (BAF) is a biological wastewater treatment process that has been used successfully for carbon oxidation, nitrification and denitrification (Peladan et al., 1996; Pujol et al., 1994; Rogalla et al., 1990; Stensel et al., 1988). BAFs are high-rate, upflow or downflow attached growth systems that incorporate submerged media responsible for supporting biofilm growth and filtering unwanted suspended solids. Attached growth, or fixed-film systems are compact treatment processes due to their retention of a dense biomass matrix. BAF systems ensure a small reactor footprint by eliminating the need for secondary clarification. Without clarification, BAFs can be operated independent of sludge settling parameters that often govern the design and operation of conventional activated sludge systems. BAFs have been shown to operate successfully under much higher hydraulic and organic loadings as compared to activated sludge systems (Metcalf and Eddy, 1991; Peladan et al., 1996; Stensel et al., 1988). While BAF systems are implemented widely in Europe, acceptance of the process is still limited in the United States. However, interest is growing, especially in areas where limited land is available for new or expanded facitilites.

One important aspect of substrate removal in fixed-film systems like BAFs is mass transfer of substrate across the bulk liquid/biofilm boundary resistance layer. Unfortunately, mass transfer in packed bed systems is not completely understood. Many attempts have been made to measure and model mass transfer in fixed-film systems (Beg et al., 1995; Horn and Hempel, 1995; Rittmann and McCarty, 1980; Zhang and Bishop, 1994). Mass transfer in fixed-film systems occurs through molecular and turbulent diffusion. Operationally, mass transfer is important because it has the potential to be the rate limiting step in substrate utilization. Additionally, it is known that mass transfer resistance can be reduced by increasing turbulence in the bulk solution (Horn and Hempel, 1995; Zhang and Bishop, 1994).

During this study, a two stage BAF pilot plant system incorporating carbon oxidation and nitrification was operated for 10 months on site at a domestic wastewater treatment facility. It was

hypothesized that it is possible to increase substrate removal at higher hydraulic loading rates due to improvements in mass transfer rates. This study sought to 1) demonstrate the effect that applied liquid velocity would have on the removal of ammonia in the second stage of a nitrifying BAF pilot system, and 2) apply an established biofilm model in an attempt to explain results from a mechanistic perspective.

EXPERIMENTAL METHODS

Pilot Plant Set-up

Two pilot-scale biological aerated filter (BAF) reactors were erected on site at the Pepper's Ferry Regional Wastewater Treatment Facility (PFRWTF) in Radford, Va., which receives a mixture of domestic and light industrial wastewater. The reactors, which were provided by Infilco Degremont, Inc. (Richmond, VA), are upflow BAFs utilizing a dense, submerged expanded clay support media 2-3 mm in diameter with an average specific surface area of 1400 m^2/m^3. A schematic of the pilot system is shown in Figure 1. The pilot system consisted of two columns that were configured in series to separate the processes of organic carbon biodegradation and nitrification. Water and air traveled in a co-current upflow fashion with backwashing also occurring in the same direction at regular intervals. Two clear well tanks continuously received and stored N column effluent to be used as backwash water. The reactors were inoculated with and continuously fed primary clarifier effluent with typical characteristics shown in Table 1.

Table. 1 Typical two-stage BAF pilot system wastewater characteristics.[a]

	Avg. Value ± S.D.[b]	
Parameter	Influent	Effluent
total BOD_5, mg/L	89±24	18±6.6
total carbonaceous BOD_5, mg/L	80±23	6.7±2.0
total COD, mg/L	242±24	54±12
soluble COD, mg/L	125±24	41±10
NH_3, mg/L as N	13±3.8	2.5±2.0
NO_2^-, mg/L as N	0.15±0.10	0.4±0.20
NO_3^-, mg/L as N	0.20±0.15	8.2±2.0
TSS, mg/L	69.6±18.1	7.6±3.5
VSS, mg/L	53.5±14.6	5.9±3.0
pH	7.3±0.2	7.0±0.1
alkalinity, mg/L as $CaCO_3$	220±66	140±45
temperature, °C	8-25°C [c]	

[a] Data collected from December 28, 1997 - September 2, 1998.
[b] S.D. = standard deviation
[c] Range of temperatures throughout study, with a summer avg. = 20°C and winter avg. = 12°C

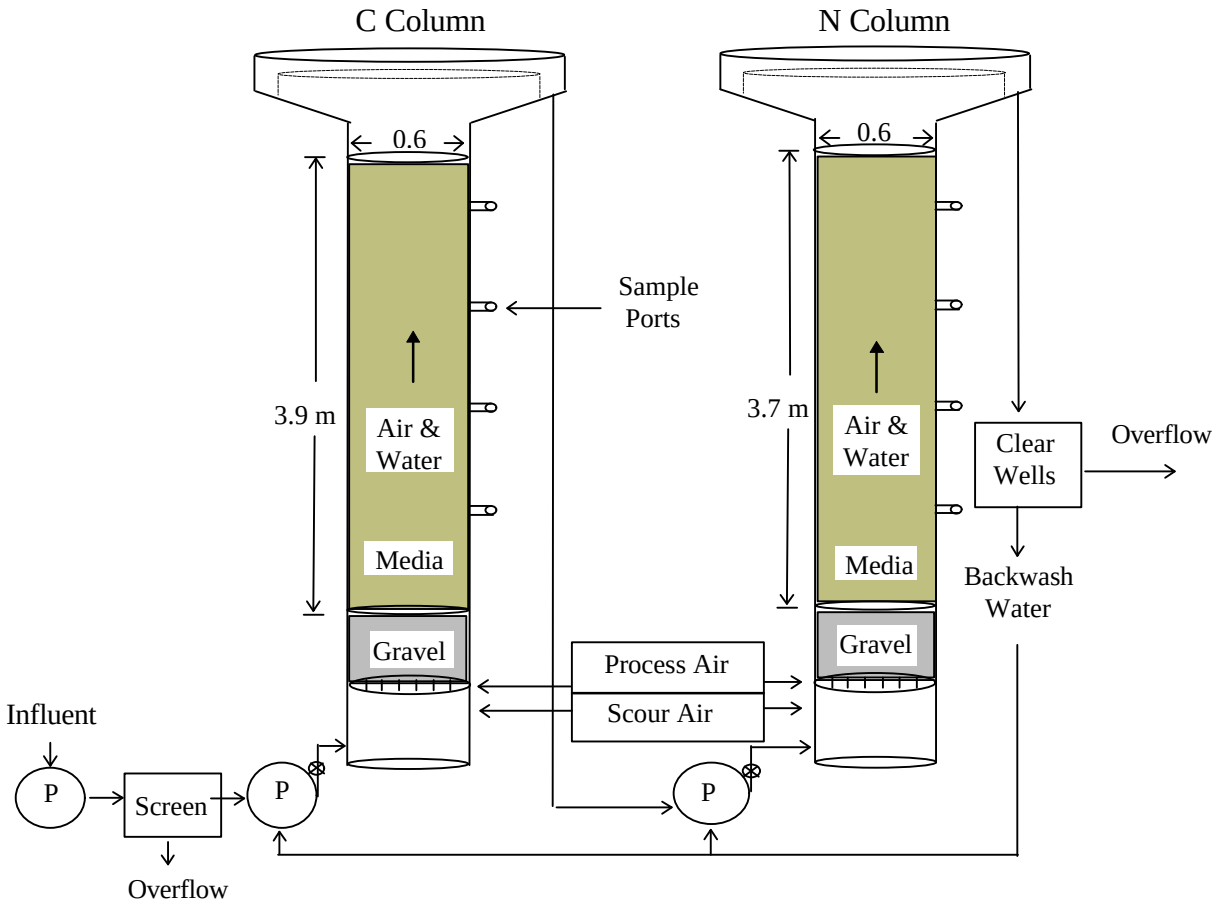

Figure 1. Two-stage BAF pilot plant schematic. (P = pump)

Abiotic Tracer Studies

Inert tracer tests using sodium chloride (NaCl) were conducted over a range of hydraulic and air flow rates prior to inoculation of the reactors. Effluent salt concentration was measured at one minute intervals with a conductivity probe. Tracer tests were performed in a step-wise fashion and were allowed to continue until effluent salt concentration was stable. The majority of the tests were conducted on the N column, but select tests were duplicated on the C column. Tracer tests were also performed on two isolated sections of the column that contained no media: 1) a section of column beneath the air distribution system but above the water inlet (approximately 285 L), and 2) the effluent collection area above the media bed but below the overflow (approximately 470 L).

Performance monitoring

Fully-automatic operation and data collection began on December 29, 1997 and continued through November 3, 1998. Refrigerated composite samplers were used to collect samples of the pilot system influent, C column and N column effluent on either a 1 or 2 hr interval over a 24 hr period. The samples were analyzed for pH, TSS, VSS, total BOD_5 carbonaceous BOD_5 ($cBOD_5$), soluble COD, NH_3-N, NO_2-N, and NO_3-N four times per week. For $cBOD_5$ analysis, nitrification was inhibited using HACH Nitrification Inhibitor Formula 2533 (trichloromethylpyridine). Once a week, samples were analyzed for total and soluble TKN, total COD, and alkalinity. All analyses were performed according to Standard Methods (AHPA, 1995), and specific methods are listed in Table A1. Soluble samples for COD, TKN, and ammonia analysis were prepared by filtering samples through 1.5 micron glass fiber filters (Whatman Type 934/AH). Ion samples (NO_2-N, NO_3-N) were prepared by filtering through 0.45 micron Supor membrane filters (Gelman Scientific), and ion analysis was measured using a Dionex DX-120 ion chromatograph equipped with a Dionex 4600 integrator. Chloride was present in high levels (> 150 mg/L) and inhibited nitrite peak interpretation. Therefore, chloride was removed by equipping the IC injection syringe with an All-Tech Maxi-Clean IC-Ag cartridge (part no. 30266) followed by a Dionex OnGuard-H cartridge (part no. 39596). On a daily basis, operational data including air and water flow rates, compressed air temperature and pressure, column headloss, and water and ambient temperature (including a minimum and maximum reading) were recorded. Typical pilot plant effluent characteristics are shown in Table 1.

Hydraulic Loading Rate Experiments

Preliminary experiments were conducted on a laboratory scale using a core sample of media taken from the N column that was placed in a continuous upflow miniature plexi-glass column and fed N column influent. The diameter of the minicolumn was 2” and the height of media was 5”. Dissolved oxygen concentration of the influent ranged between 4-5 mg/L. After the biofilm had developed for two weeks,

influent and effluent dissolved oxygen concentrations were measured with a YSI Model 5905 BOD probe over a range of applied velocities. From these measurements, the total mass uptake of oxygen across the minicolumn was calculated for each flow rate.

Full-scale hydraulic loading tests were conducted by applying a constant ammonia mass loading (Phase 1: 1.40 ± 0.08 kg NH_3-N/m^3-d; Phase 2: 1.31 ± 0.02 kg NH_3-N/m^3-d) and a relatively constant $cBOD_5$ loading (0.65 ± 0.2 kg/m^3-d) over a range of applied water velocities (5.1 to 15.8 m/h). The target loading rates were 1.3 kg NH_3-N/m^3-d and < 0.8 kg $cBOD_5$/m^3-d. Concentrations of ammonia and $cBOD_5$ under these loading conditions ranged from 15-40 mg/L NH_3-N and 7-15 mg/L $cBOD_5$. Phases of testing were defined by the background hydraulic loading rate applied to the system (Phase 1: 8.3 m/h; Phase 2: 7.1 m/h) at which the reactors were allowed to reach a steady effluent quality for at least one week prior to testing. Because consistent $cBOD_5$ and ammonia effluent concentrations could not be expected from the C column over the range of applied flow rates, it was necessary to operate the N column independent of the C column using a controlled influent source throughout each hydraulic test.

On a given test day, effluent from the N column was collected in two 840 gallon clear well tanks that were plumbed together. Once full, the effluent flow that supplied the tanks was diverted to the waste stream. Sufficient mixing within and between both tanks was provided by submersible pumps and/or paddle mixing. Initial grab samples of the source water were collected from each tank and taken back to the Virginia Tech laboratory in a cooler (15 minutes) to be analyzed for ammonia, alkalinity, pH and TOC. Upon returning to the pilot plant site after initial sample analysis, a composite sample of well-mixed source water from both tanks was taken to represent the initial water quality characteristics ("Tank 0"). Then, depending upon the velocity to be applied and the initial ammonia concentration in the source water, ammonium chloride (NH_4Cl) salt was added to the source water to supply the necessary concentration for a 1.3 kg/m^3-d ammonia loading. Sodium bicarbonate ($NaHCO_3$) was also added to bring the initial alkalinity in the source water above 300 mg/L as $CaCO_3$ to prevent alkalinity limitations due to nitrification. To avoid

nitrification inhibition by heterotrophic bacteria, the organic loading was kept below 0.8 kg $cBOD_5/m^3$-d by diluting the source water with tap water as necessary. The dilution ratio was based on preliminary TOC measurements. Finally, because it was assumed that a chlorine residual of 0.5 mg/L was likely to be present in the dilution water, sodium sulfite ($NaSO_2$) was added in stoichiometric amounts to the source water to eliminate the chlorine. After chemical addition and dilution, the tanks were mixed and a composite sample of water grabbed from both tanks was taken ("Tank 1").

Additional submersible pumps located in each tank were plumbed to the N column influent box that supplied water to the influent pump. The N column was continuously operated on the C column effluent until initiation of the hydraulic test when the C column effluent would be diverted to the waste stream. Influent flows were adjusted, and sampling began once flows were steady. The air supply was held constant at 7 scfm for each test, which was sufficient to provide nearly two times the stoichiometric oxygen requirement, assuming a 15 percent O_2 transfer efficiency.

Depending upon the applied flow rate, the test duration ranged from 90-180 minutes. Sampling throughout the tests consisted of effluent grab samples every 10-20 minutes and an effluent composite over the last third of the test period. Two additional source water composite samples were taken during the first half of the test ("Tank 2", "Tank 3"). Samples were stored and transported on ice to the Virginia Tech laboratory. Prior to filtration, source water samples and effluent composites were set up for BOD_5 and $cBOD_5$ analysis. All samples were then filtered through 1.5 micron glass fiber filters, and the filtrate of the source water samples, composites and select grab samples were analyzed for pH, alkalinity, NO_3^- and NO_2^-. All filtered samples were then preserved with sulfuric acid (pH<2) and refrigerated for future ammonia analysis.

One variation of the test setup involved conducting tests in a step-wise fashion. Each tank was prepared with a different concentration of ammonia so that the applied velocity could be changed after the volume of water in one tank was used. This allowed for minimization of daily variables during the hydraulic loading tests such as background pilot plant performance and changes in PFRWTF performance.

Model Application

A biofilm model initially developed by Williamson and McCarty (1976) and improved upon by Rittmann and McCarty (1980) and Saez and Rittmann (1987) was applied to the data collected in this study to ascertain whether the observed performance results correlate with the fundamental phenomena and assumptions that form the basis of the biofilm model. The model offers a pseudo-analytical solution for steady state biofilm kinetics through which substrate flux into a biofilm can be obtained from simple algebraic expressions that require only kinetic and physical parameters and a bulk substrate concentration (Saez and Rittmann, 1987). The model considerations and assumptions include a) biological reaction based on Monod kinetics, b) application of Fick's law for diffusion of substrate across the bulk liquid/biofilm boundary and within the biofilm, c) a total biofilm mass balance including growth, decay and shear losses, d) a homogeneous biofilm matrix with uniform local cell density and thickness, e) one limiting substrate that changes only in the direction perpendicular to the biofilm surface, f) all required nutrients (other than the one specified to be limiting) are in excess concentrations, and g) a steady-state biofilm, which is defined as a biofilm that is not growing or decaying over time (Rittmann and McCarty, 1980).

Detailed discussions of the equations governing the model can be found in the literature (Rittmann and McCarty, 1980; Saez and Rittmann, 1987). The pseudo-analytical solution expresses the flux, J^*_b, into a biofilm of any thickness as a fraction, *f*, of the substrate flux into a deep biofilm, $J^*_{b,\ deep}$. (Parameters denoted with a * are dimensionless). The factor *f* is the ratio between the fluxes into the actual and deep biofilms for the same substrate concentrations and kinetic parameters.

$$J^*_b = f \cdot J^*_{b,deep} \qquad \text{[Eq. 1]}$$

$$f = \tanh\left[\alpha\left(\frac{S_s^*}{S_{min}^*} - 1\right)^{\beta}\right] \qquad \text{[Eq. 2]}$$

$$J^*_{b,deep} = \left\{2\left[S_s^* - \ln\left(1 + S_s^*\right)\right]\right\}^{1/2} \qquad \text{[Eq. 3]}$$

S_{min}* is the threshold bulk substrate concentration below which no significant biofilm activity occurs, and can be computed from the biofilm loss coefficient, b', the half maximum-rate substrate concentration, K_s, the maximum specific substrate utilization rate, k, and the true yield coefficient, Y as

$$S_{min} = \frac{K_s b'}{Yk - b'} \qquad \text{[Eq. 4]}$$

The dimensionless substrate concentration at the diffusion layer/biofilm interface, S_s*, is not usually known, but is related in this model to the dimensionless bulk substrate concentration S_b* and can be solved by trial and error from Eq. 5.

$$S_b^* = S_s^* + \frac{\tanh[\alpha\left(\frac{S_s^*}{S_{min}^*} - 1\right)^{\beta}\left\{2\left[S_s^* - \ln\left(1 + S_s^*\right)\right]\right\}^{1/2}}{K_L^*} \qquad \text{[Eq. 5]}$$

K_L* is the dimensionless mass transfer coefficient, and α and β are functions of S_{min}*

The kinetic parameters used in the model were obtained from typical values reported in the literature for nitrifying biofilms and are summarized below in Table 2. Mass transfer coefficients were estimated using correlation equations found in the literature (Christiansen et al., 1995; Zhang and Bishop, 1994) and derived from the model by correlating the observed experimental flux to the flux predicted by the model. Experimental flux was calculated by performing a mass balance on ammonia along the N column, which resulted in Eq.6.

$$J = U_A \frac{A_s}{A_m}\left(C_o - C_e\right) \qquad \text{[Eq. 6]}$$

where U_A = velocity applied to the column, [LT^{-1}]
A_s = column surface area, [L^2]
A_m = media surface area, [L^2]
C_o = initial substrate concentration, [ML^{-3}]
C_e = effluent substrate concentration, [ML^{-3}]

The flux predicted by the model was an average flux that was based on inlet and outlet bulk ammonia concentrations.

The model was also applied to two data sets collected during normal pilot operation on August 6 and September 1, 1998, in which the columns were operating under steady-state conditions at hydraulic loading rates of 8.2 and 9.0 m/h, respectively. On these dates, ammonia concentration profiles were measured along the height of the column by sampling from liquid ports located at approximately 20, 40, 60 and 80% intervals. The column was divided into five sections based on sample port locations, and the overall mass flux of ammonia into the biofilm was calculated for each section. The known bulk substrate influent and effluent concentrations for each section were then used in the model to predict an average flux for each column section. Again, K_L values for each column section were derived from the model by fitting the model flux predictions to the observed experimental flux.

Table 2. Kinetic parameters used in model application.

	Parameter	Units	Value
b	specific decay	hr^{-1}	0.0021[a]
b_{det}	specific loss to shearing	hr^{-1}	0.0013[a]
b'	total biofilm loss rate ($=b+b_{det}$)	hr^{-1}	0.0034[a]
Y_A	true yield coefficient	mg VSS/mg N	0.2[a]
q_A	maximum specific substrate uptake rate	mg N/mg VSS-hr	0.179[a]
$X_{f,A}$	biofilm density	mg VSS/cm^3	12.7[a]
D	molecular diffusion coefficient of substrate in liquid	$cm^{2/}hr$	0.031
D_f	effective molecular diffusion of substrate in biofilm	$cm^{2/}hr$	0.027[b]
K_s	half-maximum-rate substrate concnetration	mg/cm^3	0.001_b

[a]Rittmann and Manem (1992).
[b]Grady et al. (1999).

RESULTS AND DISCUSSION

N Column Operational Performance

Ammonia removal during the summertime operational period was dependent on the ammonia-N mass loading. For hydraulic loading rates of 7.9 - 9.0 m/h, 80-100% removal was consistently achieved up to a mass loading of 0.8 kg NH_3-N/m^3-d[a]. However, performance declined at a hydraulic loading rate of 10.6 m/h to as low as 65% removal, even at mass ammonia loadings of 0.8 kg NH_3-N/m^3-d. Figure 2 offers an explanation for this decline by showing the influence of carbonaceous BOD_5 loading applied to the N column on ammonia removal during the same operation period. Once $cBOD_5$ mass loadings exceeded 1.2 kg/m^3-d, ammonia removal on average fell below 90%. The poor nitrification performance exhibited by the system in the summertime with a 10.6 m/h hydraulic loading rate could have been due to the increased presence of heterotrophic bacteria in the N column as a result of high $cBOD_5$ mass loadings. In a study conducted on the same pilot system by Gilmore et al. (1998), oligonucleotide probing conducted on biomass samples from the N column during two phases of operation with total BOD_5 loadings of 1.5 ±0.3 and 2.7±0.2 kg/m^3-d showed that a greater fraction of the recovered RNA was attributed to heterotrophic activity in the samples collected under high BOD_5 loading conditions. Additionally, Rogalla et al. (1990) found during a BAF pilot study that the maximum nitrogen removal rate started to decrease when COD loading approached 4 kg/m^3-d, which would be comparable to a BOD_5 loading of 1.6 kg/m^3-d assuming a typical domestic COD to BOD_5 ratio of 2.5:1. Because it is clear that a high organic mass loading influences nitrifying BAF systems, an effort was made to keep the $cBOD_5$ loading below 0.8 kg/m^3-d during the hydraulic loading experiments.

Influence of Hydraulic Loading on Nitrification

The mixing regime of both the C and N columns can be described as a plug flow bed of media preceded and followed by a well-mixed portion of the column that contains no media. The initial CSTR is

[a] volumetric mass loading and removal rates defined per bioreactor bed volume.

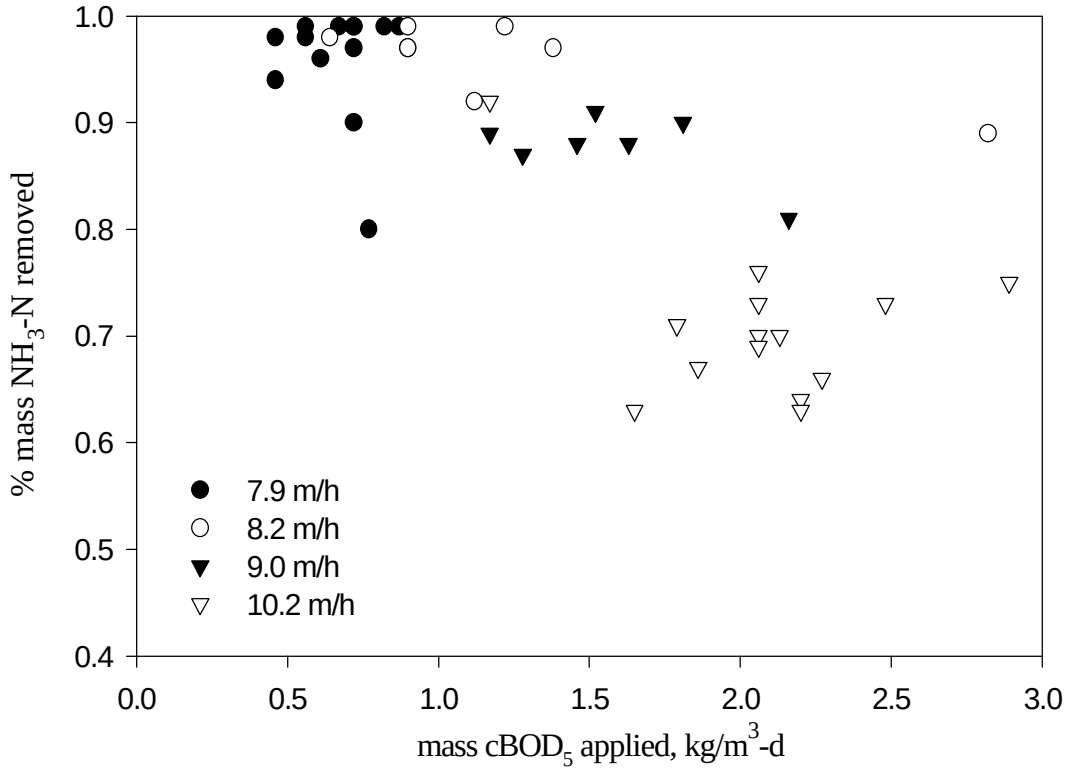

Figure 2. Influence of $cBOD_5$ loading on N column nitrification performance over a range of hydraulic loadings during summer operation.

created by empty column space, approximately 75 gallons, under the air diffusers but above the water inlet, while the CSTR following the media bed represents mixed effluent that sits above the media, approximately 125 gallons, before flowing over the weir (see Figure 1). Inert tracer studies were conducted on the columns prior to inoculation. An example of the data collected from the tracer tests at a hydraulic loading rate of 10.3 m/h and an air flow rate of 8 scfm is illustrated in Figure 3. Figure 3 also shows the effluent ammonia data collected during three of the hydraulic loading rate experiments and illustrates the effluent stability achieved during the testing period. Each test, including the tracer test, reached stability after approximately three plug flow residence times in the N column.

Nitrification performance during each test was evaluated on a mass ammonia removal basis once a steady-state effluent quality was achieved. Nitrification inhibition by heterotrophic activity in the N column was kept to a minimum by controlling the $cBOD_5$ mass loading during the tests (0.65 ± 0.2 kg $cBOD_5/m^3$-d). The influence of hydraulic loading rate, or upflow water velocity, on the mass ammonia removal observed during both phases of testing is illustrated in Figure 4. Duplicate tests were performed during phase 2 for upflow velocity conditions of 5.1, 7.9, and 10.3 m/h, and error bars on Figure 4 represent standard deviation. Phase 1 originally consisted of four velocity conditions. However, due to the recycle of extraordinarily high ammonia from biosolids dewatering at PFRWTF during the 24-hr period prior to the test day, the data set at 10.3 m/h was eliminated. A statistical analysis of the data sets reveals that the slope of the phase 2 data set is significantly greater than zero ($P=0.0136$, $\alpha=0.05$), while the slope of the phase 1 data set is not ($P=0.3249$, $\alpha=0.5$). Due to the duplicate tests and the greater number of data points in the phase 2 data set, more confidence is placed on the phase 2 results.

During phase 2 the mass of ammonia-N nitrified increased approximately 17% as velocity increased from 5.1 m/h to 15.8 m/h. Peladan et al. (1996) conducted a pilot study on a single-stage BAF system in which a synthetic wastewater containing ammonia and inorganic carbon was applied over a similar range of velocities (5 and 20 m/h). The results from their study show a strikingly similar percent

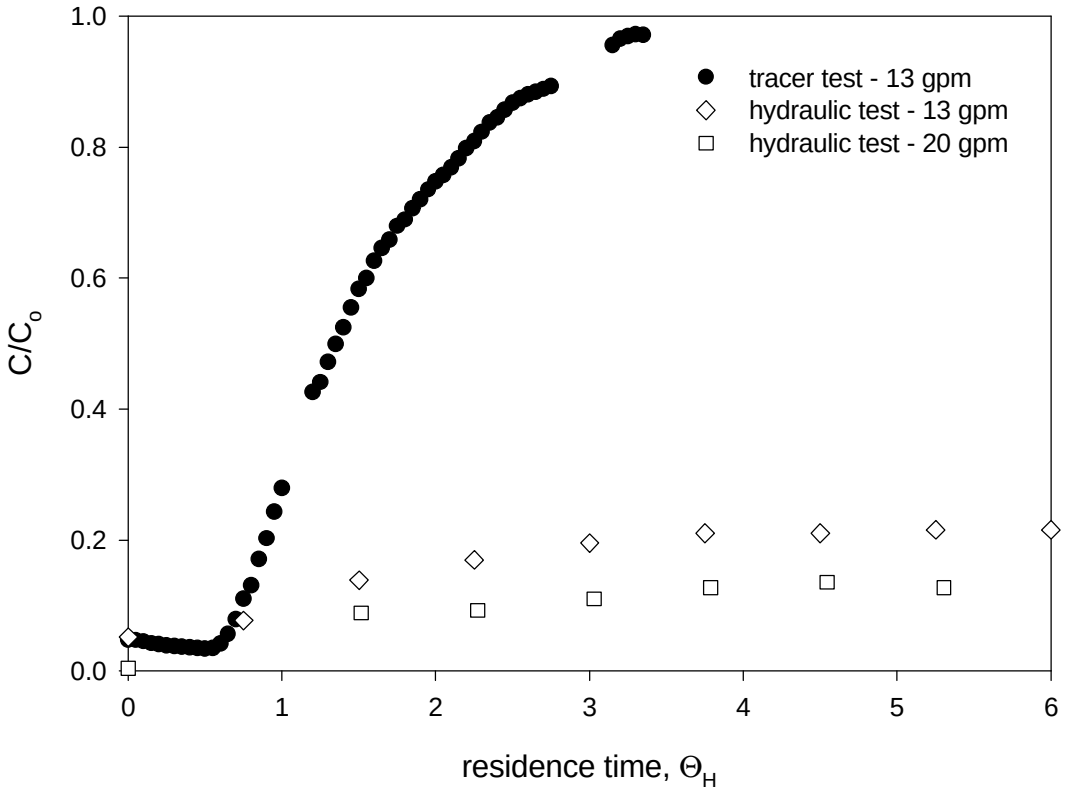

Figure 3. Effluent profiles from abiotic tracer test and hydraulic loading rate experiments. Residence time is based on plug flow reactor contact time.

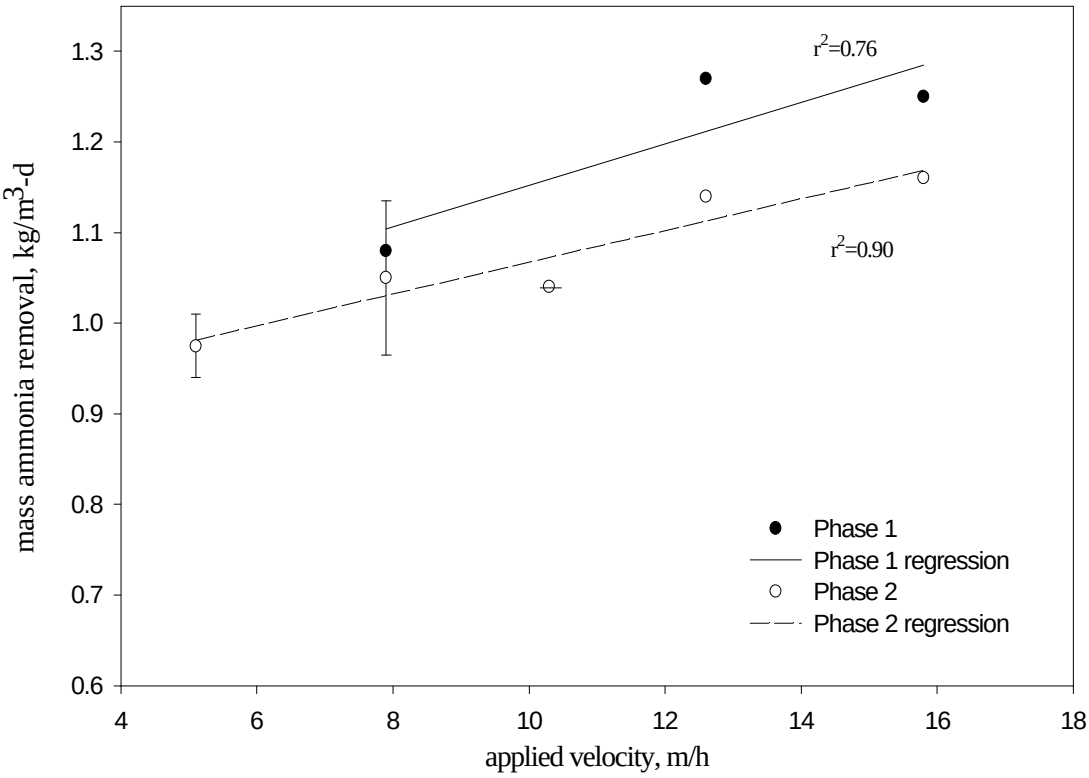

Figure 4. Influence of upflow velocity on mass ammonia removal during hydraulic loading experiments. Applied ammonia load: Phase 1 = 1.33-1.53 kg/m^3-d; Phase 2 = 1.28-1.32 kg/m^3-d. Error bars represent standard deviation.

increase in nitrification of 19%. Peladan et al. (1996) acknowledged the value of conducting additional high rate nitrification studies on systems using domestic wastewater. According to the study presented here, the effects of the presence of organic material is revealed in the magnitude of the mass of ammonia removed. Whereas Peladan et al. (1996) were able to remove approximately 3 kg NH_3-N/m^3-d, the highest removal achieved in this study was 1.26 kg NH_3-N/m^3-d. Peladan et al. (1996) also investigated nitrification at velocities as high as 30 m/h, although their data suggests that little to no improvement in the mass of ammonia removed could be seen above a hydraulic loading rate of 15 m/h.

A comparison of nitrification performance from normal summertime operation over a range of hydraulic loading rates and the nitrification performance observed during the hydraulic experiments is shown in Figure 5. This figure illustrates two important points clarified by the hydraulic experiments. First, $cBOD_5$ mass loading limits the nitrification performance in the second stage of this system. The data at 10.6 m/h during normal operation were obtained under high $cBOD_5$ mass loadings (1.5 to 3.0 kg/m^3-d) and high NH_3-N mass loadings (0.8 to 1.1 kg/m^3-d) and show that performance clearly declined. Data from phase 2 of the hydraulic experiments represent an even higher NH_3-N loading (1.3 kg/m^3-d) under minimized $cBOD_5$ mass loading (less than 0.8 kg/m^3-d), and show an improvement in performance. Second, nitrification performance improves with higher upflow water velocities. The ammonia removal during phase 2 shown in Figure 5 improves from 76% to 85% ammonia removal as velocity is increased.

Other studies have been conducted in which the effect of fluid velocites on biofilm performance has been investigated (Debus et al, 1994; Kugaprasathan et al., 1992; Zhang and Bishop, 1994). Kugaprasatham et al. (1992) in particular examined the effect of turbulence on nitrifying biofilms and also found an increase in mass flux of ammonia-N with increasing bulk liquid turbulence. They hypothesized that the flux is influenced by turbulence because of the changes that result in both substrate diffusion and biofilm structure under more turbulent conditions. Similarly, Debus et al. (1994) observed higher levels of degradation by biofilms with increased fluid velocities. Based on measurements of dissolved oxygen

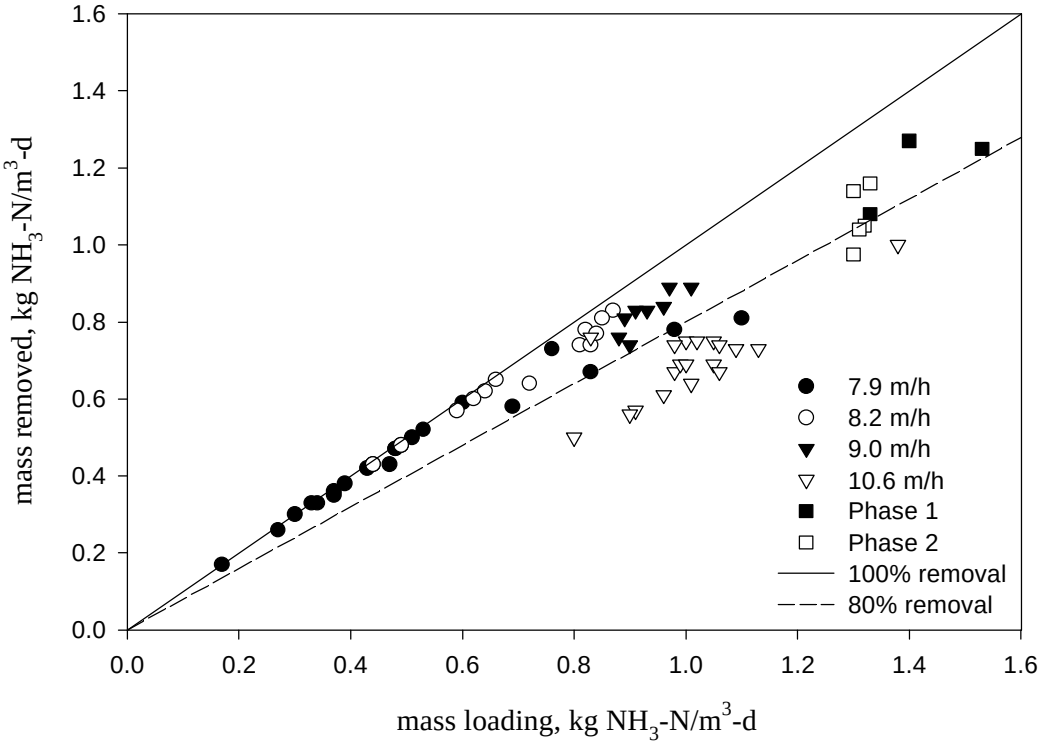

Figure 5. Comparison of ammonia removal performance during normal N column summer operation over a range of hydraulic loading rates and the hydraulic testing period.

concentrations at the bulk/biofilm interface, it was concluded that boundarylayer thickness had decreased at higher velocities resulting in faster substrate transfer (Debus et al., 1994).

Biofilm Model Application

Measurements of physical biofilm characteristics such as boundary layer thickness or structural properties were not obtained in this study, so conclusions about the fundamental phenomena governing the observed improvement in performance were difficult to develop. Instead, a pseudo-analytical biofilm model presented by Saez and Rittmann (1987) was applied to the data collected in this study to ascertain whether the observed nitrification performance results correlate with the fundamental phenomena and assumptions that form the basis of the biofilm model The model was used to derive K_L values for each hydraulic loading rate by correlating the flux predicted by the model with the experimental flux calculated with Eq. 6. These inferred K_L values were then compared with K_L values obtained from correlation equations (Christiansen et al., 1995; Zhang and Bishop, 1994). Variability between the K_L values derived from the model and from the correlation equations could represent differences in mass transfer but could also be explained by other characteristics of the pilot system. K_L values inferred from the model and obtained from correlation equations for different hydraulic loading rates are shown on Figure 6.

The model was also applied to two data sets collected during normal pilot operation in which ammonia concentration was monitored at intervals along the height of the N column. The known bulk substrate influent and effluent concentrations for each column interval were used in the model to predict an average flux. Again, K_L values were derived from the model so that the experimental flux, calculated by Eq. 6, correlated with the model results. Fitted K_L values varied throughout each column section, and the average K_L value for each of the two data sets, along with the standard deviation, are also presented on Figure 6.

Figure 6 shows that the K_L values inferred from the model as applied to the data from the hydraulic loading rate experiments are lower than those predicted using two different correlation equations.

However, the rate of increase in mass transfer with velocity is similar for all three data sets. Neither of the two correlation equations represent the exact experimental conditions. For example, the correlation developed by Christiansen et al. (1995) was based only upon fundamental fluid mechanics in a packed bed where no biofilm is present. Zhang et al. (1994) present a theoretical correlation developed for a biofilm grown on a flat surface rather than in a packed bed. It is likely that such differences in reactor configuration will affect mass transfer, but because the K_L values were derived from the model rather than directly measured, the variation seen in Fig. 6 could also be representing other factors that the model did not address.

Since the velocity throughout the column is constant for any given hydraulic loading rate, the model assumes that K_L is constant. However, when K_L values at different intervals along the length of the column were inferred from the model and averaged, a large standard deviation resulted, as seen in Fig. 6. There was a general trend to the variation in that the derived K_L values tended to increase with column height. It cannot be concluded that K_L does in fact vary with column height. Instead, it is possible that the variability in the inferred K_L values is actually accounting for other changes throughout the column that the model fails to address, such as variation in biofilm kinetics and structure. For example, the model used in this study is based on a single limiting substrate. However, organic matter is also eliminated in the N column. Depending upon the performance of the C column, which precedes the N column in this two-stage process, the organic loading to the N column varies. It would be expected that due to the initially high heterotrophic activity measured at the lower portions of the N column by Gilmore et al. (1998), the flux of ammonia into the biofilm is actually greater in the middle and upper portions of the column. This could explain why K_L values that were derived using the model increased with height. Additionally, it is very likely that the biofilm density changes throughout the height of the column. According to Peyton (1995), biofilm density decreases as substrate loading decreases. As ammonia is removed throughout the length of the reactor, the substrate loading and the density are possibly decreasing. According to the model, a

decrease in density predicts a higher flux. If the model could account for the variability in biomass density throughout the reactor, less variation in derived K_L values would have resulted.

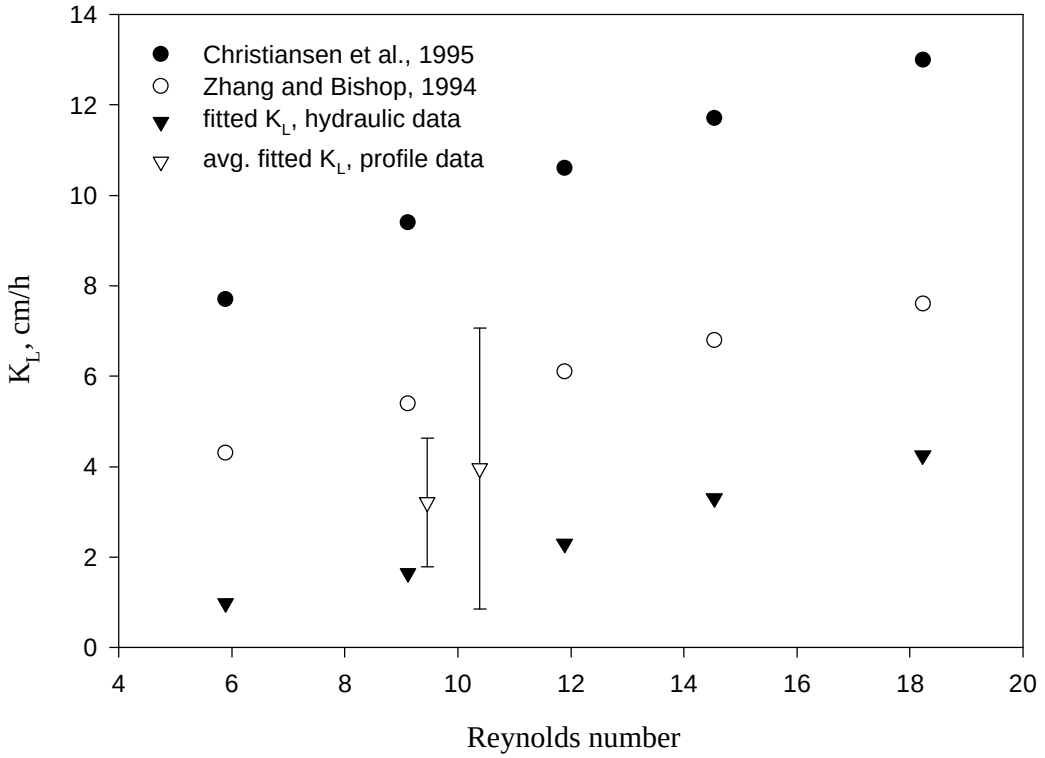

Figure 6. Comparison of K_L values derived from the biofilm model and two different correlation equations. Error bars represent standard deviation.

CONCLUSIONS

The results of this study demonstrate that a modest improvement in nitrification performance in a pilot-scale, submerged-media biological aerated filter occurs with increased hydraulic loading conditions. The results may indicate that full-scale BAF systems similar to the system studied here can be designed for higher hydraulic loading rates, resulting in smaller reactor footprints. This study also demonstrated that nitrification performance in this system could only be improved with increased hydraulic rates when organic carbon loading was kept to a minimum. This implies that in order to optimize nitrification performance under high flow rates, the upstream treatment for organic carbon removal, whether it be a preceding BAF stage or an activated sludge system, must also be optimized to ensure that an increase in organic loading to the nitrifying reactor does not accompany increased hydraulic loading rates. In other words, nitrifying BAF system designs cannot be based solely on hydraulic loading rate. Because this pilot system was operated at a variety of hydraulic flow rates, organic loading rates and ammonia loading rates, it has the potential to serve as an independent assessment of the performance capability of a two-stage, nitrifying, granular media BAF system under a variety of operating conditions

The biofilm model application was not successful in determining the fundamental phenomena responsible for the improvement in nitrification performance seen at increased hydraulic loading rates. Based on the large variability in K_L values derived from the model using the experimental data and K_L values offered by correlation equations, it can only be concluded that the model does not completely describe the physical and biological characteristics of this fixed-film pilot system. More detailed measurements, including interfacial substrate concentrations, biofilm thickness and biofilm density at varying flow conditions, which would require a more controlled and thus less applicable experimental set-up, are necessary to evaluate the relationship between mass transfer and nitrification performance.

REFERENCES

APHA, AWWA, WEF. (1995). Standard methods for the examination of water and wastewater. 19th edition. Washington D.C.

Beg., S.A., Hassan, M.M., Chaudry, A.S. (1995). Multi-substrate analysis of carbon oxidation and nitrification in an unpflow packed-bed biofilm reactor. *J. Chem. Tech. Biotechnol.*, **64**, 367-378.

Christiansen, P., Hollesen, L., Harremoes, P. (1995). Liquid film diffusion on reaction rate in submerged biofilters. *Wat. Res.*, **29**, 947-952.

Debus, O., Baumgartl, H., Sekoulov, I. (1994). Influence of fluid velocities on the degradation of volatile aromatic compounds in membrane bound biofilms. *Wat. Sci. Tech.*, **29**, 253-262.

Gilmore, K.R., Husovitz, K.J., Holst, T., Love, N.G. (1998). Influence of organic and ammonia loading on nitrifier activity and nitrification performance for a two-stage biological aerated filter system. *IAWQ Specialty Conference on Microbial Ecology of Biofilms: Concepts, Tools and Applications*, Lake Bluff, IL.

Grady, C.P.L., Jr., Daigger, G.T., Lim, H.C. (1999). *Biological Wastewater Treatment*. Marcel Dekker, Inc. New York.

Horn, H. and Hempel, D.C. (1995). Mass transfer coefficients for an autotrophic and a heterotrophic biofilm system. *Wat. Sci. Tech.*, **32**, 199-204.

Kugaprasathan, S., Nagaoka, H., Ohgaki, S. (1992). Effect of turbulence on nitrifying biofilms at non-limiting substrate conditions. *Wat. Res.*, **26**, 1629-1638.

Metcalf and Eddy, Inc. (1991). Wastewater Engineering: Treatment, Disposal and Reuse. 3rd edition. McGraw Hill, Inc., New York, NY.

Peladan, J.G., Lemmel, H., Pujol, R. (1996). High nitrification rate with upflow biofiltration. *Wat. Sci. Tech.*, **34**, 347-353.

Peyton, Brent M. (1996). Effects of shear stress and substrate loading rate on *Pseudomonas aeruginosa* biofilm thickness and density. *Wat. Res.*, **30**, 29-36.

Pujol., R., Hamon, M., Kandel, X., Lemmel, H. (1994). Biofilters: Flexible, reliable biological reactors. *Wat. Sci. Tech.*, **29**, 33-38.

Rittmann, B.E. and Manem, J.A. (1992). Development and experimental evaluation of a steady-state, multispecies biofilm model. *Biotechnol. Bioeng.*, **39**, 914-922.

Rittmann, B.E. and McCarty, P.L. (1981). Substrate flux into biofilms of any thickness. *J. Evniron. Engr.*, **107**, 831-847.

Rogalla, F., Payraudeau, M., Bacquet, G., Bourbigot, M., Sibony, J., Gilles, P. (1990). Nitrification and phosphorus precipitation with biological aerated filters. *Journal WPCF*, **62**, 169-176.

Saez, P. and Rittman, B.E. (1987). Improved pseudoanalytical solution for steady-state biofilm kinetics. *Biotechnol. Bioeng*., **32**, 379-385.

Saez, P. and Rittmann, B.E. (1990). Error analysis of limiting-case solutions to the steady-state biofilm model. *Wat. Res*., **24**, 1181-1185.

Stensel, H.D., Brenner, R.C., Lee, K.M., Melcer, H., Rakness, K. (1988). Biological filter evaluation. *J. Evniron. Engr*., **114**, 655-671.

Williamson K. and McCarty, P.L. (1976) A model of substrate utilization by bacterial films. *Journal WPCF*, **48**, 9-23.

Zhang, T.C. and Bishop, P.L. (1994). Experimental determination of the dissolved oxygen boundary layer and mass transfer resistance near the fluid-biofilm interface. *Wat. Res*., **30**, 47-58.

ENGINEERING SIGNIFICANCE

Biological aerated filter systems are implemented widely in European countries, yet they have not gained full acceptance the United States. However, the numerous advantages that BAFs offer are beginning to attract treatment facilities and design engineers to this treatment option. The primary advantages offered by BAF systems are a reduced footprint resulting from the elimination of secondary clarifiers, elimination of sludge settling issues, and a low treatment time due to the high biomass concentration. It is because of these advantages that BAFs present an ideal solution for upgrading and expanding existing wastewater treatment facilities where available space is limited.

The first full-scale two-stage BAF system in the United States is currently being installed in Roanoke, VA as part of the facility upgrade and expansion. The same BAF technology used in this study, the Biofor™, manufactured by Infilco Degremont, Inc., is being implemented at the Roanoke treatment plant. The Biofor™ reactors will operate parallel to the existing activated sludge process and are designed to provide an additional average treatment capacity of 10 MGD. The first stage will consist of 6 Biofor C cells, each at 1034 ft^2 (96 m^2) with 12.8 (3.9 m) ft of media. The second stage will consist of 6 Biofor N cells, each at 640 ft^2 (59.5 m^2) with the same media height. Under average flow conditions, the first stage of operation will see a hydraulic loading of 1.1 gpm/ft^2 (2.7 m/h), and the second stage will be loaded at a rate of 1.8 gpm/ft^2 (4.4 m/h). Given the typical average influent wastewater characteristics at average flow conditions, 2.8 kg BOD_5/m^3-d will be applied to the Biofor C. Assuming 70% removal of the BOD_5 in the first stage of operation, the Biofor N cells will receive on average an organic loading of 1.4 kg BOD_5/m^3-d and an ammonia loading of approximately 0.65 kg/m^3-d. Under winter conditions with a minimum temperature of 10°C, over 90% of the applied ammonia load must be removed.

The pilot system performance presented in this study as well as by Love et al. (1998) demonstrated successful operation, which was defined by the same effluent quality parameters that must be met at the Roanoke wastewater facility, at hydraulic rates that were twice as great as that specified for the new

Roanoke facility. The best average $cBOD_5$ mass removal efficiency in the Biofor C (78 ± 5%) occurred at a hydraulic loading rate of 9.0 m/h with applied $cBOD_5$ mass loadings ranging from 1.5 to 4.4 kg/m^3-d (Love et al., 1999). Nearly complete nitrification at ammonia mass loadings as high as 0.7 kg/m^3-d was consistently achieved at hydraulic loading rates up to 8.2 m/h. This implies that there may have been the potential to design the Roanoke facility to receive higher hydraulic loadings so that reactor area along with cost could have been reduced. However, this study also emphasized that high organic loading rates can hinder Biofor N nitrification performance. One design parameter, such as hydraulic loading, should not be the governing parameter for the design of these two-stage systems. Many factors combined, including organic and ammonia loading rates, hydraulic loading rates and temperature, will determine the performance capability of the system. Pilot-scale testing is the best aid to evaluate performance under a variety of operating conditions. Since pilot testing is not always feasible, this study, as an independent assessment of the performance capability of a two-stage, granular media BAF system under a variety of operating conditions, can serve as a guide for future BAF designs.

REFERNCES

Love, N.G., Gilmore, K.R., Husovitz, K.J., Delahaye, A.P., Novak, J.T., Little, J.C. (1999)
Performance of a two-stage biological aerated filter system treating domestic wastewater for BOD_5, ammonia and TSS removal - pilot plant results. Submitted to WEFTEC 1999.

APPENDIX A: EXPERIMENTAL METHODS

Table A1. Standard Methods Used For Water Quality Analysis

Analysis	*Standard Method*	*Description*
Ammonia	4500-NH_3 B & C	Preliminary distillation and titrimetric method
BOD_5/$cBOD_5$	5210 B	5-day BOD test
COD	5220 C	Closed reflux, titrimetric method
TKN	4500-N_{org}	Macro-Kjeldahl method
TSS	2540 D	TSS dried at 103-105°C
VSS	2540 E	VSS dried at 550°C
Alkalinity	2320 B	Titration method

APPENDIX B: RAW DATA

Table B1. Operational Data: Ammonia Removal Performance, Summer Period

Date	hydraulic loading (m/h)	influent NH_3-N (mg/L)	effluent NH3-N (mg/L)	mass applied (kg/m^3-d)	mass removed (kg/m^3-d)	% rem (by mass)
4/8	7.9	13.4	2.1	0.69	0.58	0.84
4/9		19.2	3.9	0.98	0.78	0.80
4/13		10.4	0.2	0.53	0.52	0.98
4/16		21.4	5.6	1.10	0.81	0.74
4/20		3.4	0.1	0.17	0.17	0.97
4/23		5.2	0.1	0.27	0.26	0.98
4/27		8.5	0.1	0.44	0.43	0.99
4/30		9.9	0.1	0.51	0.50	0.99
5/4		7.6	0.1	0.39	0.38	0.99
5/6		6.5	0.1	0.33	0.33	0.98
5/11		5.9	0.1	0.30	0.30	0.98
5/13		6.6	0.1	0.34	0.33	0.98
5/18		8.3	0.1	0.43	0.42	0.99
5/27		9.2	0.9	0.47	0.43	0.90
5/30		7.2	0.4	0.37	0.35	0.94
6/1		7.2	0.1	0.37	0.36	0.99
6/3		9.3	0.1	0.48	0.47	0.99
6/4		9.3	0.1	0.48	0.47	0.99
6/6		11.8	0.3	0.60	0.59	0.97
6/8		9.5	0.1	0.49	0.48	0.99
6/10		16.2	3.2	0.83	0.67	0.80
6/11		14.9	0.6	0.76	0.73	0.96
6/13	10.6	16.4	5.8	1.13	0.73	0.65
6/15		12	0.95	0.83	0.76	0.92
6/18		20	5.4	1.38	1.00	0.73
6/27		11.6	4.3	0.80	0.50	0.63
6/29		14.2	4.5	0.98	0.67	0.68
7/1		13.2	4.9	0.91	0.57	0.63
7/2		13.1	4.9	0.90	0.56	0.63
7/4		14	5.1	0.96	0.61	0.64
7/6		14.7	5.4	1.01	0.64	0.63
7/8		15.8	5.2	1.09	0.73	0.67
7/9		15.3	4.4	1.05	0.75	0.71
7/11		14.4	4.3	0.99	0.69	0.70
7/13		15.2	5.2	1.05	0.69	0.66
7/15		15.4	5.7	1.06	0.67	0.63
7/16		14.6	4.5	1.00	0.69	0.69
7/18		14.6	3.7	1.00	0.75	0.75
7/20		15.4	4.6	1.06	0.74	0.70
7/22		14.9	4	1.02	0.75	0.73
7/23		14.3	3.5	0.98	0.74	0.76

Table B1. (cont.) Operational Data: Ammonia Removal Performance, Summer Period

Date	hydraulic loading (m/h)	influent NH_3-N (mg/L)	effluent NH3-N (mg/L)	mass applied (kg/m^3-d)	mass removed (kg/m^3-d)	% rem (by mass)
7/25	9	15	2	0.88	0.76	0.87
7/27		16	1.8	0.93	0.83	0.89
7/29		15.5	2.9	0.90	0.74	0.81
7/30		15.6	1.4	0.91	0.83	0.91
8/1		16.4	2	0.96	0.84	0.88
8/3		16.7	1.4	0.97	0.89	0.92
8/5		17.3	2	1.01	0.89	0.88
8/7		15.3	1.5	0.89	0.81	0.90
8/10	8.2	8.2	0.1	0.44	0.43	0.99
8/12		9.2	0.14	0.49	0.48	0.98
8/13		12.1	0.4	0.64	0.62	0.97
8/15		13.5	1.5	0.72	0.64	0.89
8/17		11.1	0.3	0.59	0.57	0.97
8/19		11.7	0.4	0.62	0.60	0.97
8/20		12.4	0.17	0.66	0.65	0.99
8/22		15.2	1.2	0.81	0.74	0.92
8/23		15.6	1.7	0.83	0.74	0.89
8/26		15.5	0.77	0.82	0.78	0.95
8/27		15.7	1.14	0.84	0.77	0.93
8/29		16.4	0.76	0.87	0.83	0.95
8/31		16	0.74	0.85	0.81	0.95

Table B2. Operational Data: $cBOD_5$ Removal Performance, Summer Period

Date	hydraulic loading (m/h)	influent cBOD (mg/L)	effluent cBOD (mg/L)	mass applied (kg/m^3-d)
4/8	7.9	20	4	1.02
4/9		17	6	0.87
4/13		10		0.51
4/16		14	8	0.72
4/20		6	5	0.31
4/23				
4/27		9	8	0.46
4/30		9	5	0.46
5/4		14	5	0.72
5/6		11	2	0.56
5/11				
5/13		9	4	0.46
5/18		17	6	0.87
5/27		14	5	0.72
5/30		9	4	0.46
6/1		11	5	0.56
6/3		16	4	0.82
6/4		13	4	0.67
6/6		14	5	0.72
6/8		14	4	0.72
6/10		15	6	0.77
6/11		12	4	0.61
6/13	10.6			
6/15		17	4	1.17
6/18		30	5	2.06
6/27			8	
6/29				
7/1				
7/2				
7/4		32	8	2.20
7/6		24	6	1.65
7/8		27	7	1.86
7/9		26	5	1.79
7/11		30	6	2.06
7/13		33	7	2.27
7/15		32	11	2.20
7/16		30	10	2.06
7/18		42	10	2.89
7/20		31	9	2.13
7/22		36	11	2.48
7/23		30	8	2.06

Table B2 (cont.). Operational Data: $cBOD_5$ Removal Performance, Summer Period

Date	hydraulic loading (m/h)	influent cBOD (mg/L)	effluent cBOD (mg/L)	mass applied (kg/m^3-d)
7/25	9	22	7	1.28
7/27		20	7	1.17
7/29		37	12	2.16
7/30		26	6	1.52
8/1		28	9	1.63
8/3				
8/5		25	8	1.46
8/7		31	10	1.81
8/10	8.2	17	3.4	0.90
8/12		12	3.5	0.64
8/13		17	5	0.90
8/15		53	7	2.82
8/17		17	6	0.90
8/19		26	7	1.38
8/20		23	6	1.22
8/22		21	6	1.12

Table B3. Hydraulic Loading Rate Experiments: Raw Data

Test date	Phase	Hydraulic loading (m/h)	Sample	NH3-N (mg/L as N)	COD (mg/L)	BOD (mg/L)	cBOD (mg/L)	pH	alkalinity (mg/L as $CaCO_3$)	NO_3^- (mg/L as N)
9/18/98	1	7.9	Tank 0	1.8	49	19	6.3	6.82		13.7
			Tank 1	26	56	38	7.7	7.2	306	13.4
			0	5.9				6.8		18.4
			20	6.5				6.8		20.0
			40	5.6				6.82	157	26.1
			60	5.2				6.83		31.3
			80	4.8				6.93		32.9
			100	4.6				6.9		32.8
			120	4.5				6.9	149	33.8
			140	5				6.95		31.9
			160	5.1				6.94		32.7
			180	5				6.98	153	31.1
			Comp 1	5		13	3.2	7.18		
			Comp 2	5.4	45			7.12		33.8
9/29/98	1	10.3	Tank 0		43	28	9	6.71	70	12.1
			Tank 1	20.4	48	47	10	7.3	241	12.2
			Tank 2	20.3						
			Tank 3	20.5						
			N eff	9.2						
			0	9.5						
			20	8						
			40	2.9				6.6	104	
			60	1.3						31.2
			80	0.6				6.65	102	
			100	1						
			120	1				6.71	108	29.5
			Comp 1	1.4						
			Comp 2	0.8	42	16	6.0			29.4

Table B3 (cont.). Hydraulic Loading Rate Experiments: Raw Data

Test date	Phase	Hydraulic loading (m/h)	Sample	NH3-N (mg/L as N)	COD (mg/L)	BOD (mg/L)	cBOD (mg/L)	pH	alkalinity (mg/L as $CaCO_3$)	NO_3^- (mg/L as N)
9/26/98	1	12.6	Tank 0	0.74	40	29	8.3	6.93	122	8.1
			Tank 1	16.5	42	30	7.6	7.35	302	7.8
			Tank 2	18.1						
			Tank 3	16.7						
			N eff	0.2						
			0	0.2						
			15	0.6						
			30	0.9				7.02	180	
			45	1.2						19.5
			60	1.4						
			75	1.6						
			90	1.7						
			105	1.5						22.9
			Comp 1	1.4				7.22	186	
			Comp 2	1.6	43	18	5.7	6.9	190	18.5
9/21/98	1	15.8	Tank 0	0.3	19	31	12	7.05		5.5
			Tank 1	14.9	21	62	8.5	7.5	277	5.4
			N eff	1.1				6.84		
			0	1.3				6.75		
			10	2.3				6.78		
			20	2.3				6.87		
			30	2.5				6.95	191	
			40	2.5				6.87		15.8
			50	2.5				6.88		
			60	2.6				6.9	199	
			70	2.6				6.87		
			80	2.8				7		
			90	2.7				6.96	201	15.2
			Comp 1	2.5				6.98		
			Comp 2	2.8	20		5.0	7.03		13.3

Table B3 (cont.) Hydraulic Loading Rate Experiments: Raw Data

Test date	Phase	Hydraulic loading (m/h)	Sample	NH3-N (mg/L as N)	COD (mg/L)	BOD (mg/L)	cBOD (mg/L)	pH	alkalinity (mg/L as $CaCO_3$)	NO_3^- (mg/L as N)
10/13/98	2	7.9	Tank 0	0.7	45	19	7.5	6.95	90	13.1
			Tank 1	25.9	54	54	9.5	7.39	296	13.2
			Tank 2	25.3						
			Tank 3	25.6						
			N eff.	5.2						
			0	5.4						
			20	6.3				6.8	118	
			40	6.6						
			60	6.6				6.87	128	31.0
			80	6.7						
			100	6.4						
			120	6.2						
			150	6.3				6.95	130	31.1
			Comp	6.4	44	19	5.0			27.6
10/19/98	2	7.9	Tank 0	0.3	49	22	6.4	6.82	100	14.7
			Tank 1	26	53		11.7	7.25	280	14.7
			Tank 2	26.3				7.4		
			Tank 3	25.7				7.45		
			N eff.	2.9				6.65	98	
			0	3.2				6.72		
			20	4.2				6.74	105	24.2
			40	4.3				6.8		
			60	4.3				6.85	120	35.2
			80	4.3				6.76		
			100	4.3				6.78		
			120	4.3				6.8		
			150	4.3				6.8	120	36.8
			Comp	4.3	53	28	5.1	6.72		35.8

Table B3 (cont.) Hydraulic Loading Rate Experiments: Raw Data

Test date	Phase	Hydraulic loading (m/h)	Sample	NH3-N (mg/L as N)	COD (mg/L)	BOD (mg/L)	cBOD (mg/L)	pH	alkalinity (mg/L as $CaCO_3$)	NO_3^- (mg/L as N)
10/15/98	2	10.3	Tank 0	1.2	38	31	9.7	6.59	68	8.7
			Tank 1	19.8	41		14	7.33	308	8.9
			Tank 2	19.8				7.41		
			Tank 3	19.6				7.38		
			N eff.	1				6.5		
			0	1				6.53		
			15	1.5				6.65		
			30	2.7				6.68	150	21.9
			45	3.3				6.87		
			60	3.8				6.82		
			75	4.1				6.87	182	23.7
			90	4.1				6.86		
			105	4.2				6.83		
			120	4.2				6.86	184	24.0
			Comp	4.4	39	28	6.3	6.89	180	23.0
10/20/98	2	12.6	Tank 0	0.44	32	23	7.9	6.87	78	10
			Tank 1	16	32		7.9	7.3	288	10.2
			Tank 2	15.9				7.28		
			Tank 3	15.6						
			N eff.	4.6						
			0	4.3				6.61	120	
			15	4						
			30	3.7				6.78	170	
			45	2.7						25.6
			60	2.1				6.79	176	
			75	1.9				6.78		
			90	1.9				6.78		23.3
			105	1.9				6.75	178	
			Comp	1.8	31	25	4.2	6.92		23.8

Table B3. (cont.) Hydraulic Loading Rate Experiments: Raw Data

Test date	Phase	Hydraulic loading (m/h)	Sample	NH3-N (mg/L as N)	COD (mg/L)	BOD (mg/L)	cBOD (mg/L)	pH	alkalinity (mg/L as $CaCO_3$)	NO_3^- (mg/L as N)
11/3/98	2	15.8	Tank 0	0.6	19	32	8.7	7.2	54	5.7
			Tank 1	12.75	21		10.7	7.83	274	5.7
			Tank 2	13.2						
			N eff.	0.1						
			0	0.05						
			20	1.15				6.93	154	16.5
			30	1.2						
			40	1.43						
			50	1.65						
			60	1.76				7.18	198	17.2
			70	1.65						
			80	1.76						
			90	1.6	16			7.25	194	16.4
			comp	1.7			10.2			15.8

Table B3 (cont.) Hydraulic Loading Rate Experiments: Raw Data

Step-wise test 1: 5.1 - 10.3 m/h

Test date	Phase	Hydraulic loading (m/h)	Sample	NH3-N (mg/L as N)	COD (mg/L)	BOD (mg/L)	cBOD (mg/L)	pH	alkalinity (mg/L as $CaCO_3$)	NO_3^- (mg/L as N)
10/23/98	2	5.1	Tank 0	0.38	40.1	31	12.5	7.25	88	10.4
			Tank 1	38.3	38.6		15	7.72	400	10.1
			Tank 2	40.6						
			N eff	0.27						
			0	0.22						
			20	0.11						
			40	0.77				6.83	114	
			60	3.2						29.9
			80	5.9						
			100	8.6						
			120	9.3	34.7	13	5	7	182	36.4
			comp	8.1						33.4
		10.3	Tank 0	0.38	30.1	22	8	7.2	80	9.5
			Tank 1	19.7	40.9		7	7.62	294	9.5
			Tank 2	19.2						
			N eff							
			0	9.6						
			10	13.1						
			20	12.8				7.1	210	
			30	9.3						28.6
			40	7						
			50	5.4						
			60	4.3				7.13	180	25.4
			70	3.9	33.2	16	4			
			comp	5.6						25.6

Table B3 (cont.). Hydraulic Loading Rate Experiments: Raw Data

Step-wise test 2: 5.1 - 15.8 m/h

Test date	Phase	Hydraulic loading (m/h)	Sample	NH3-N (mg/L as N)	COD (mg/L)	BOD (mg/L)	cBOD (mg/L)	pH	alkalinity (mg/L as $CaCO_3$)	NO_3^- (mg/L as N)
10/27/98	2	5.1	Tank 0	0.55	33	49	18			
			Tank 1	38.8	32.2		14	7.57	390	10.3
			Tank 2	42.8						
			N eff							
			0	0.16						
			20	0.17						20
			40							
			60	4.9				6.7	244	29.7
			80	7.8						
			100	9.8				6.86	170	
			120	10.3				6.83	172	36.2
			124	10.4	27.5		5.4			
		15.8	Tank 0							
			Tank 1	12.8				7.66	314	6.6
			Tank 2							
			N eff							
			0	10.4						
			10	16.1						
			20	9.8				7	250	20.9
			30	5.6						
			35							
			40	3.9						
			45	3.5				6.98	250	17.1
			48.5	3.2						

Note:

Air flow problems during 15.8 m/h test. Air lines must need cleaning because after a short shut-down between flows, air did not climb above 5.8 scfm with valve completely open.

Did not use data from this test.

Table B4. Hydraulic Loading Rate Experiments: Loading and Removal

Ammonia Data:							**BOD Data:**			
Phase	Velocity (m/h)	C_o (mg/L)	$C_{f\ (grabs)}$ (mg/L)	$C_{f\ (composite)}$ (mg/L)	Applied Load (kg/m^3-d)	Removed Load (kg/m^3-d)	C_o (mg/L)	C_f (mg/L)	Applied Load (kg/m^3-d)	Removed Load (kg/m^3-d)
1	7.9	26.0	5.0	5.4	1.33	1.08	7.7	3.2	0.39	0.23
	10.3	20.4	0.9	0.8	1.36	1.30	10	5.9	0.67	0.27
	12.6	17.1	1.6	1.6	1.40	1.27	7.6	5.7	0.62	0.16
	15.8	14.9	2.7	2.8	1.53	1.25	8.5	5.0	0.87	0.36
Phase	Velocity (m/h)	C_o (mg/L)	$C_{f\ (grabs)}$ (mg/L)	$C_{f\ (composite)}$ (mg/L)	Applied Load (kg/m^3-d)	Removed Load (kg/m^3-d)	C_o (mg/L)	C_f (mg/L)	Applied Load (kg/m^3-d)	Removed Load (kg/m^3-d)
2	5.1	39.5	9.6		1.31	0.99	15	5	0.50	0.33
	5.1	38.8	10.4		1.28	0.94	14	5.4	0.46	0.28
	7.9	25.6	6.3	6.4	1.31	0.99	9.5	5	0.49	0.23
	7.9	26.0	4.3	4.3	1.33	1.11	11.7	5.1	0.60	0.34
	10.3	19.5	3.9		1.30	1.04	14	6.3	0.94	0.51
	10.3	19.8	4.2	4.4	1.32	1.04	7	4	0.57	0.25
	12.6	15.9	1.9	1.8	1.30	1.14	7.9	4.2	0.65	0.30
	15.8	13	1.7	1.7	1.33	1.16	10.7	10.2	1.10	0.05

APPENDIX C: BIOFILM MODEL APPLICATION

Table C1. Biofilm Model Application: Constants

Kinetic Parameters			*Physical Parmaters*		
b_{det}	0.0013	hr^{-1}	D	0.031	cm^2/hr
b	0.0021	hr^{-1}	D_f	0.027	cm^2/hr
Y_A	0.2	mg VSS/mg N	υ	1.00E-06	m^2/s
q_{max}	0.179	mg N/mg VSS-hr	Sc = υ/D	465.1	
K_s	0.001	mg N/cm^3	ε	0.4	
$X_{f,A}$	12.7	mg/cm^3	ρ	998.2	kg/m^3
			d	0.0025	m

Table C2. Application of Model to Hydraulic Loading Rate Experimental Data

Constants derived from the model:

$S_B{}^*_{min}$	0.105
α	1.866
B	0.523

Calculate k_L for range of k_L values*

velocity (m/h)	k_L (cm/hr)	k_L*	S_{B0} (mg/cm^3)	S_{Be} (mg/cm^3)	S_{B0}*	S_{Be}*	Re
5.1	0.98	0.016	0.039	0.010	39.2	10	5.9
7.9	1.65	0.027	0.026	0.0053	25.8	5.3	9.1
10.3	2.30	0.037	0.020	0.004	19.7	4.05	11.9
12.6	3.30	0.054	0.016	0.0019	15.9	1.9	14.5
15.8	4.25	0.069	0.013	0.0017	13.0	1.7	18.2

*Solve iteratively for S_S**

velocity (m/h)	S_{S0}* guess	S_{B0}*	S_{B0}* target	$J_{s\ deep}$*	f	J_s *	J_s (mg/cm^2-hr)	avg J_s (mg/cm^2-hr)
5.1	0.7415	39.20995	39.2	6.11E-01	1.0	0.611	0.0048	0.003005
	0.18	9.998937	10	1.70E-01	0.9	0.156	0.0012	
7.9	0.8292	25.79939	25.8	6.71E-01	1.0	0.671	0.0053	0.003171
	0.1648	5.308742	5.3	1.57E-01	0.9	0.138	0.0011	
10.3	0.88	19.70127	19.7	7.05E-01	1.0	0.705	0.0055	0.003332
	0.1707	4.048927	4.05	1.62E-01	0.9	0.145	0.0011	
12.6	1.025	15.89126	15.9	7.99E-01	1.0	0.799	0.0063	0.003504
	0.134	1.905028	1.9	1.28E-01	0.7	0.095	0.0007	
15.8	1.068	13.00194	13	8.26E-01	1.0	0.826	0.0065	0.003659
	0.1419	1.697173	1.7	1.36E-01	0.8	0.108	0.0008	

Table C3. Profile Data from Biofor N used in Model Application

Date	N flow rate (m/h)	Port	NH_3-N (mg/L)	cBOD (mg/L)	NH_4 load (kg/m3-d)	cBOD load (kg/m3-d)
6-Aug	9	C5	16.0	31	0.93	1.8
		N1	15.5		0.90	
		N2	11.4		0.67	
		N3	6.7		0.39	
		N4	5.2		0.30	
		N5	1.5		0.09	
1-Sep	8.2	C5	17.0	26	0.90	1.4
		N1	14.3		0.76	
		N2	9.7		0.52	
		N3	5.9		0.31	
		N4	2.9		0.15	
		N5	1.6		0.09	

Table C4. Model Application: NH_3 Profile at 8.2 m/h with Variable K_L Throughout Column

velocity (m/h)	column section	k_L (cm/hr)	k_L*	S_{B0} (mg/cm^3)	S_{BE} (mg/cm^3)	S_{B0}*	S_{BE}*
8.2	1	1.15	0.019	0.017	0.014	17.0	14.3
	2	2.62	0.043	0.014	0.0097	14.3	9.7
	3	3.37	0.055	0.010	0.006	9.7	5.9
	4	4.85	0.079	0.006	0.0029	5.9	2.9
	5	4.05	0.066	0.0029	0.0016	2.9	1.6

*Solve iteratively for SS**

column section	S_{S0}* guess	S_{B0}*	S_{B0}* target	Js deep*	f	Js *	Js (mg/cm^2-hr)	avg Js (mg/cm^2-hr)
1	0.3476	17.00001	17	3.14E-01	1.0	0.312	0.0024	0.002251
	0.2901	14.3017	14.3	2.66E-01	1.0	0.263	0.0021	
2	0.6982	14.30067	14.3	5.81E-01	1.0	0.581	0.0045	0.003821
	0.4494	9.699395	9.7	3.96E-01	1.0	0.395	0.0031	
3	0.5874	9.700503	9.7	5.01E-01	1.0	0.500	0.0039	0.003156
	0.3397	5.900977	5.9	3.07E-01	1.0	0.305	0.0024	
4	0.4911	5.900675	5.9	4.28E-01	1.0	0.427	0.0033	0.0025
	0.2335	2.900063	2.9	2.17E-01	1.0	0.211	0.0017	
5	0.2007	2.901229	2.9	1.89E-01	0.9	0.178	0.0014	0.001077
	0.1349	1.600631	1.6	1.29E-01	0.7	0.097	0.0008	

Table C5. Overall Flux in Column using Mass Balance for 8.2 m/h Profile

$A_{surface}$ 0.283 m^2

A_{media} 280 m^2

U (m/h)	Column section	Co (mg/cm^3)	Ce (mg/cm^3)	mass balance Js (mg/cm^2-h)	model Js (mg/cm^2-h)	fitted KL
8.2	1	0.017	0.014	2.24E-03	2.25E-03	1.15
	2	0.014	0.0097	3.81E-03	3.82E-03	2.62
	3	0.010	0.006	3.15E-03	3.16E-03	3.37
	4	0.006	0.0029	2.49E-03	2.50E-03	4.85
	5	0.0029	0.0016	1.08E-03	1.08E-03	4.05
					avg	3.21
					sd	1.42

Table C6. Model Application: NH_3 Profile at 9.0 m/h with Variable K_L Throughout Column

velocity (m/h)	column section	k_L (cm/hr)	k_L*	S_{B0} (mg/cm^3)	S_{BE} (mg/cm^3)	S_{B0}*	S_{BE}*
9	1	2.37	0.039	0.0160	0.0155	16.0	15.5
	2	2.27	0.037	0.0155	0.0114	15.5	11.4
	3	4.00	0.065	0.0114	0.0067	11.4	6.7
	4	1.85	0.030	0.0067	0.0052	6.7	5.2
	5	9.30	0.152	0.0052	0.0015	5.2	1.5

*Solve iteratively for SS**

column section	S_{S0}* guess	S_{B0}*	S_{B0}* target	Js deep*	f	Js *	Js (mg/cm^2-hr)	avg Js (mg/cm^2-hr)
1	0.712	16.00197	16	5.90E-01	1.0	0.590	0.0046	0.004553
	0.686	15.49887	15.5	5.72E-01	1.0	0.572	0.0045	
2	0.6541	15.50147	15.5	5.49E-01	1.0	0.549	0.0043	0.003736
	0.4617	11.3999	11.4	4.05E-01	1.0	0.405	0.0032	
3	0.8531	11.40004	11.4	6.87E-01	1.0	0.687	0.0054	0.004284
	0.4641	6.700432	6.7	4.07E-01	1.0	0.406	0.0032	
4	0.2177	6.699329	6.7	2.04E-01	1.0	0.195	0.0015	0.001359
	0.176	5.200948	5.2	1.67E-01	0.9	0.151	0.0012	
5	0.8185	5.200896	5.2	6.64E-01	1.0	0.664	0.0052	0.003363
	0.2168	1.500281	1.5	2.03E-01	1.0	0.194	0.0015	

Table C7. Overall Flux in Column using Mass Balance for 8.2 m/h Profile

$A_{surface}$ 0.283 m^2

A_{media} 280 m^2

U (m/h)	Column section	Co (mg/cm^3)	Ce (mg/cm^3)	mass balance Js (mg/cm^2-h)	model Js (mg/cm^2-h)	fitted KL
9	1	0.0160	0.0155	4.55E-04	4.55E-03	2.37
	2	0.0155	0.0114	3.73E-03	3.74E-03	2.27
	3	0.0114	0.0067	4.28E-03	4.28E-03	4.00
	4	0.0067	0.0052	1.36E-03	1.36E-03	1.85
	5	0.0052	0.0015	3.37E-03	3.36E-03	9.30
					avg	3.96
					sd	3.10

VITA

Kari J. Husovitz was born in Jefferson City, Missouri on September 9, 1974 to Daryl and Betty Ann Husovitz, who both originate from Charleroi, Pennsylvania. She has lived with her family in Missouri, Connecticut, Georgia and South Carolina. In 1992 she graduated as valedictorian from Wade Hampton High School in Hampton, South Carolina. She attended Clemson University and graduated Summa Cum Laude in 1996 with a Bachelor of Science degree in Civil Engineering. She then continued her education at Virginia Tech and earned a Master of Science degree in Environmental Engineering. Kari successfully finished and defended her master's research in December of 1998. Currently she is residing in Charleston, SC where she is working for an environmental engineering consulting firm.